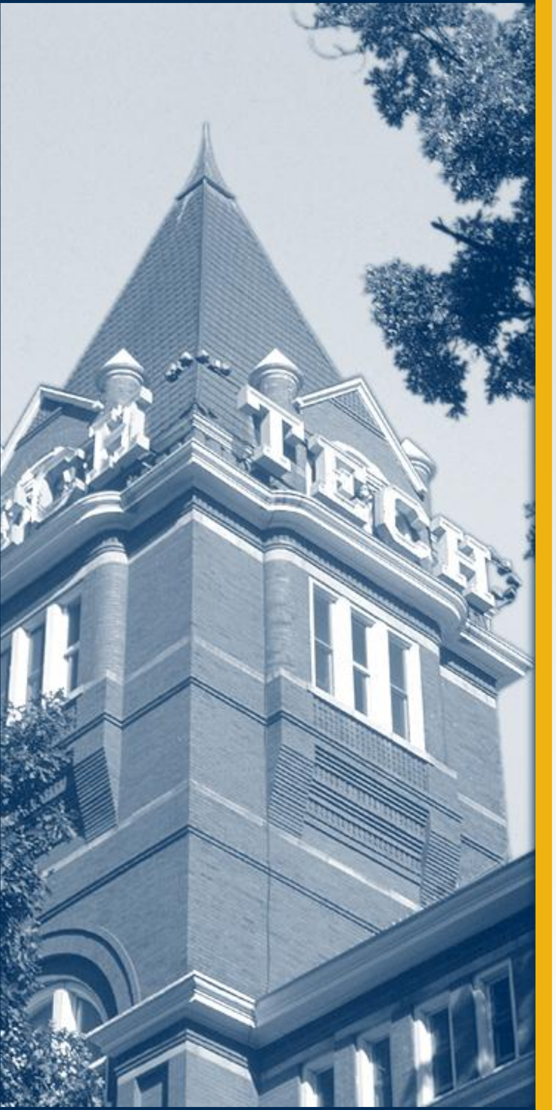

Interface Circuits and Systems for Inertial Sensors

IEEE Sensors 2013: Tutorials

November 3, 2013

Arashk Norouzpour-Shirazi

Integrated MEMS Laboratory

Georgia Institute of Technology

Contact: arashk.n@gatech.edu

Georgia Institute of Technology®

CMMT

IMEMS

MEMS Gyroscopes - Market

- Automotive applications
  - Anti-skid control

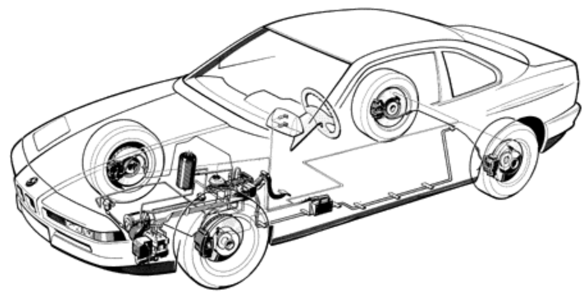

- Consumer applications
  - Image stabilization in digital cameras
  - Short-range navigation
  - Gaming consoles

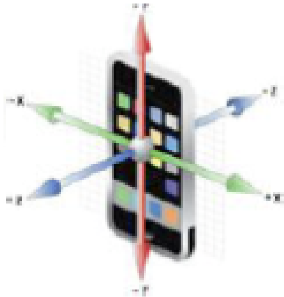

- High-performance applications
  - Aerospace
  - Defense
  - Precision inertial measurement units

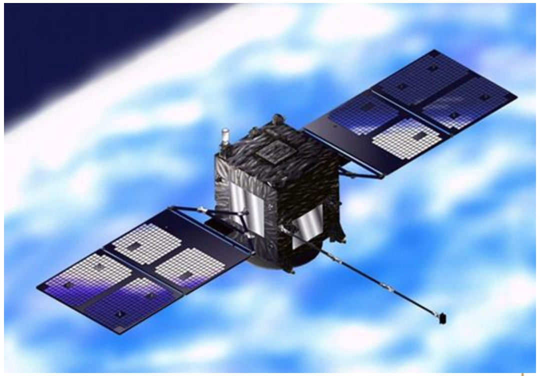

Georgia Tech

High-Performance Gyroscope Interface

- MEMS do the sensing, Circuits do the thinking!
- As MEMS gyroscopes offer lower noise levels and higher dynamic ranges, interface system noise and dynamic range must also be improved.

	Rate Grade	Tactical Grade	Inetial (Navigation) Grade
Bias drift	10 to 1000 °/hr	0.01 to 10 °/hr	<0.01 °/hr
Angle random walk	> 0.5 °/√hr	0.5 - 0.05 °/√hr	< 0.001 °/√hr
Scale factor accuracy	0.1 - 1%	100 – 1000 ppm	< 10 ppm
Full scale range	50 - 1000 °/sec	>500 °/sec	>400 °/sec
Bandwidth	> 70 Hz	~100 Hz	~100 Hz

MEMS Gyroscope - Principle of Operation

- Coriolis Effect:
  - Transfer of energy between two vibration modes
  - Deflection proportional to rotation rate

$$\vec{a}_{COR} = 2\vec{v} \times \Omega_z$$

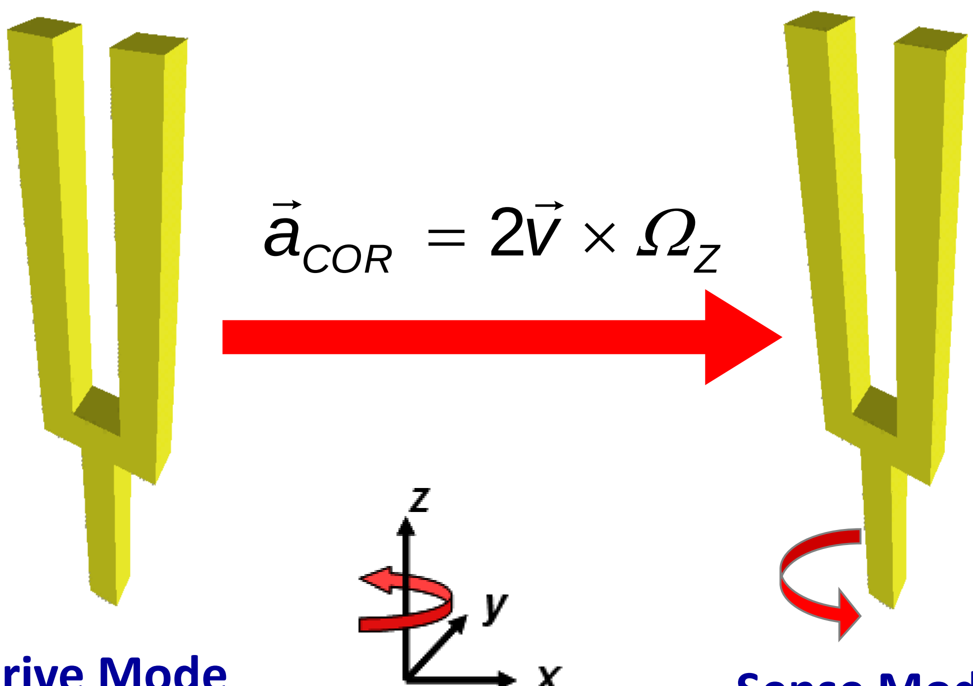

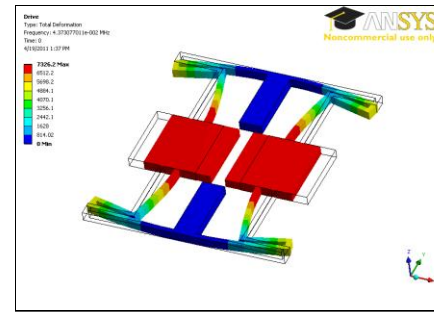

Drive Mode

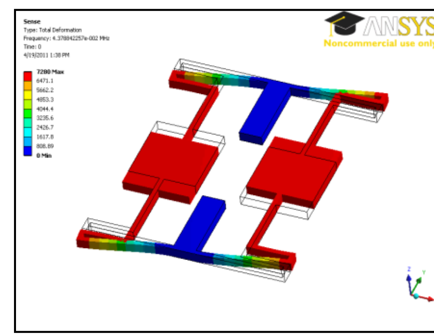

Sense Mode

Georgia Tech

Tuning-Fork Gyroscope (TFG) Model

- Gyroscope Model:
  - Mass → Motional Inductance
  - Spring → Motional Capacitance
  - Damping → Motional Resistance
- Coriolis: proportional to drive-mode velocity
- Quadrature: proportional to drive displacement (undesired signal)

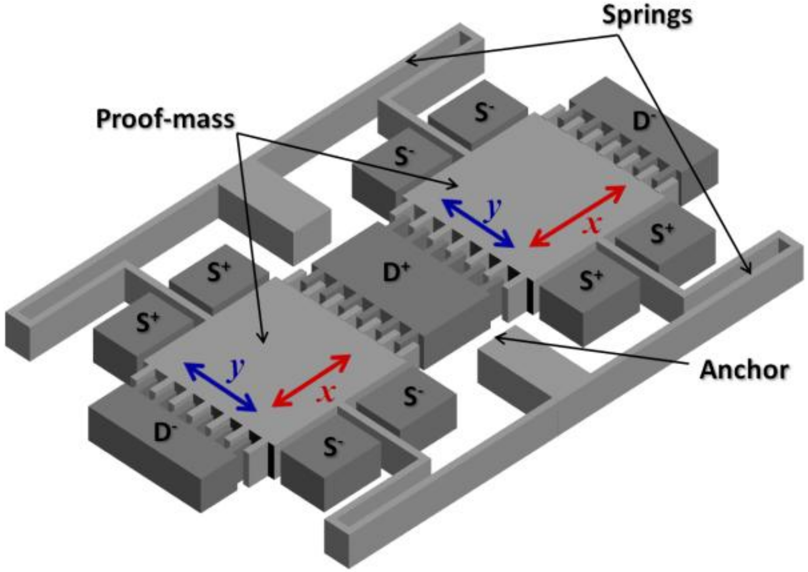

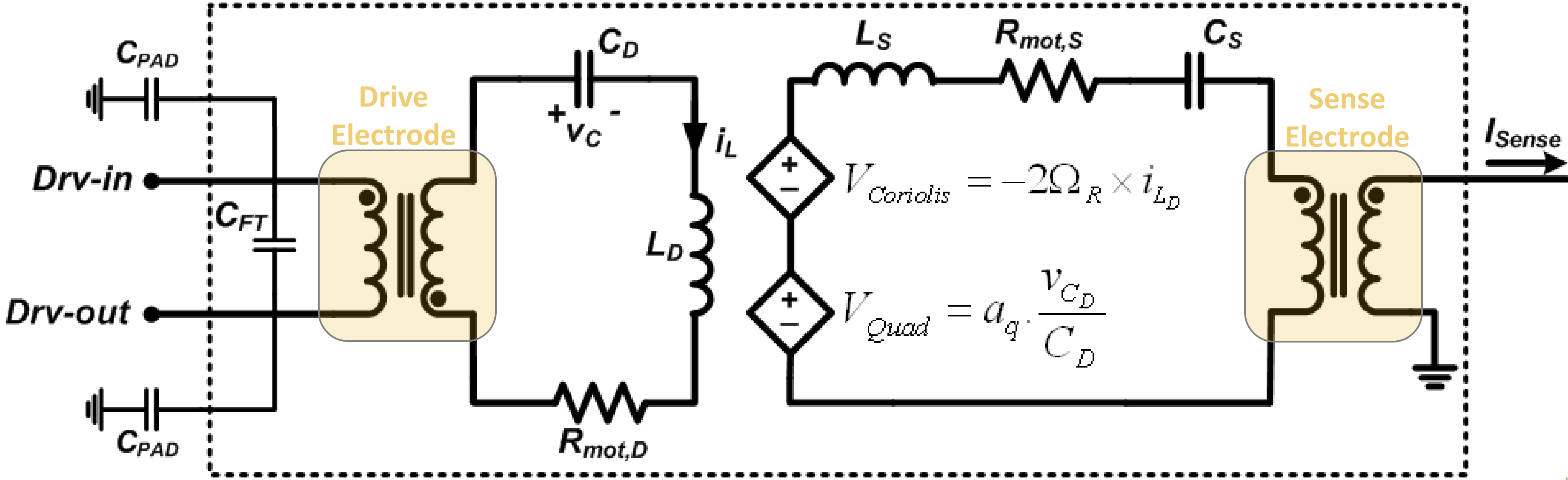

MEMS Gyroscope – Simplified Model

- Energy coupling between two modes of operation, through Coriolis force:

$$\left(s^2+\frac{\omega_D}{Q_D}s+\omega_D^2\right)X_D(s)=\frac{F_D(s)}{M},\ f_D(t)=F_D\cos\omega_D t$$

$$\left(s^2+\frac{\omega_S}{Q_S}s+\omega_S^2\right)X_S(s)=\underbrace{-2\Omega\times sX_D(s)}_{Coriolis}+\underbrace{a_Q X_D(s)}_{Quadrature}$$

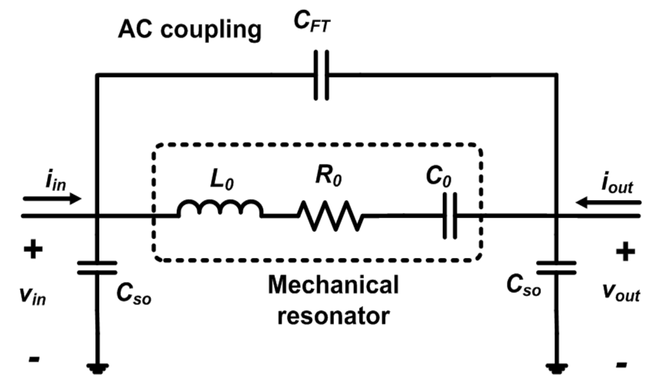

General Resonator Model

- The drive and sense signals can be derived as:

$$x_D(t)=\frac{Q_D F_D}{\omega_D^2}\sin\omega_D t,\ \dot{x}_D(t)=\frac{Q_D F_D}{\omega_D}\cos\omega_D t$$

$$x_S(t)=\frac{a_{Coriolis}\cos(\omega_D t+\varphi)+a_Q\sin(\omega_D t+\varphi)}{\omega_D\times\sqrt{(2\Delta\omega)^2+(\omega_S/Q_S)^2}},\quad \varphi=\tan^{-1}\frac{\omega_S/Q_S}{\Delta\omega}$$

- Frequency split, $\Delta\omega$ strongly affects sensitivity and phase shift of the output signals.

Georgia Tech

Mode-matching - Noise and Sensitivity

- Mode-matching improves both mechanical and electrical input-referred noise, MNEΩ and ENEΩ:

$$MNE\Omega = \frac{1}{2x_{drive}}\sqrt{\frac{4k_BT}{\omega_0 M Q_{EFF}}}.\sqrt{BW} \qquad ENE\Omega = \frac{d_{s0}}{2V_P C_{s0} Q_{EFF}\, x_{drive}}.I_{N-total}.\sqrt{BW}$$

$$\left.\frac{\Delta C}{\Omega_Z}\right|_{Matched} \propto Q_{EFF} \qquad \left.\frac{\Delta C}{\Omega_Z}\right|_{Unmatched} \propto \frac{1}{\Delta f}$$

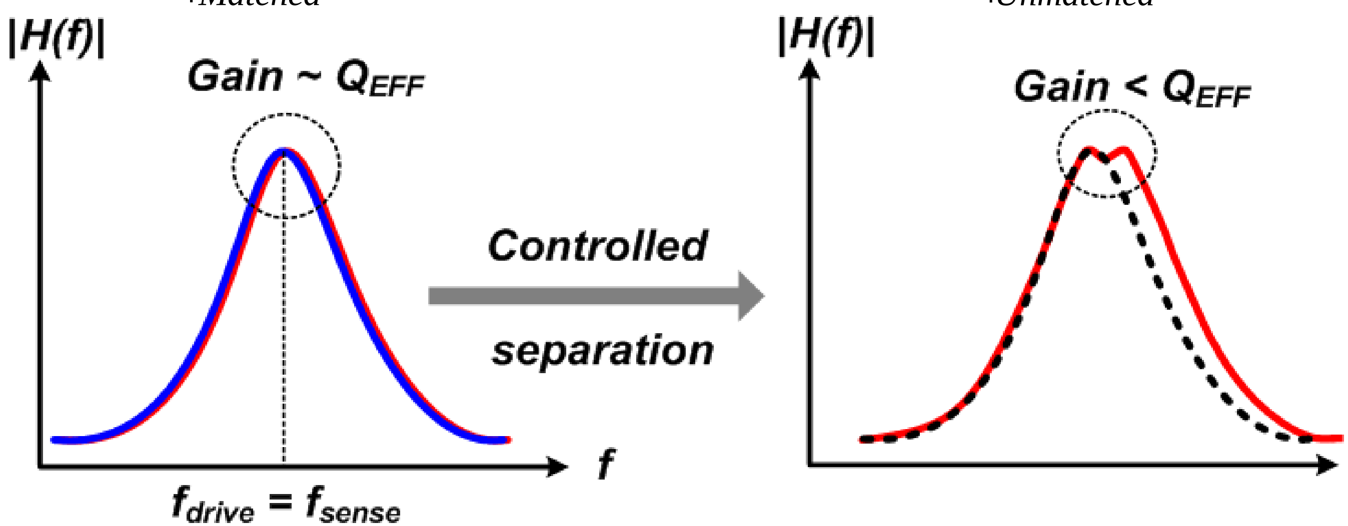

Mode-Matching

Split-mode, Low Q_{EFF} Mode-matched, High Q_{EFF}

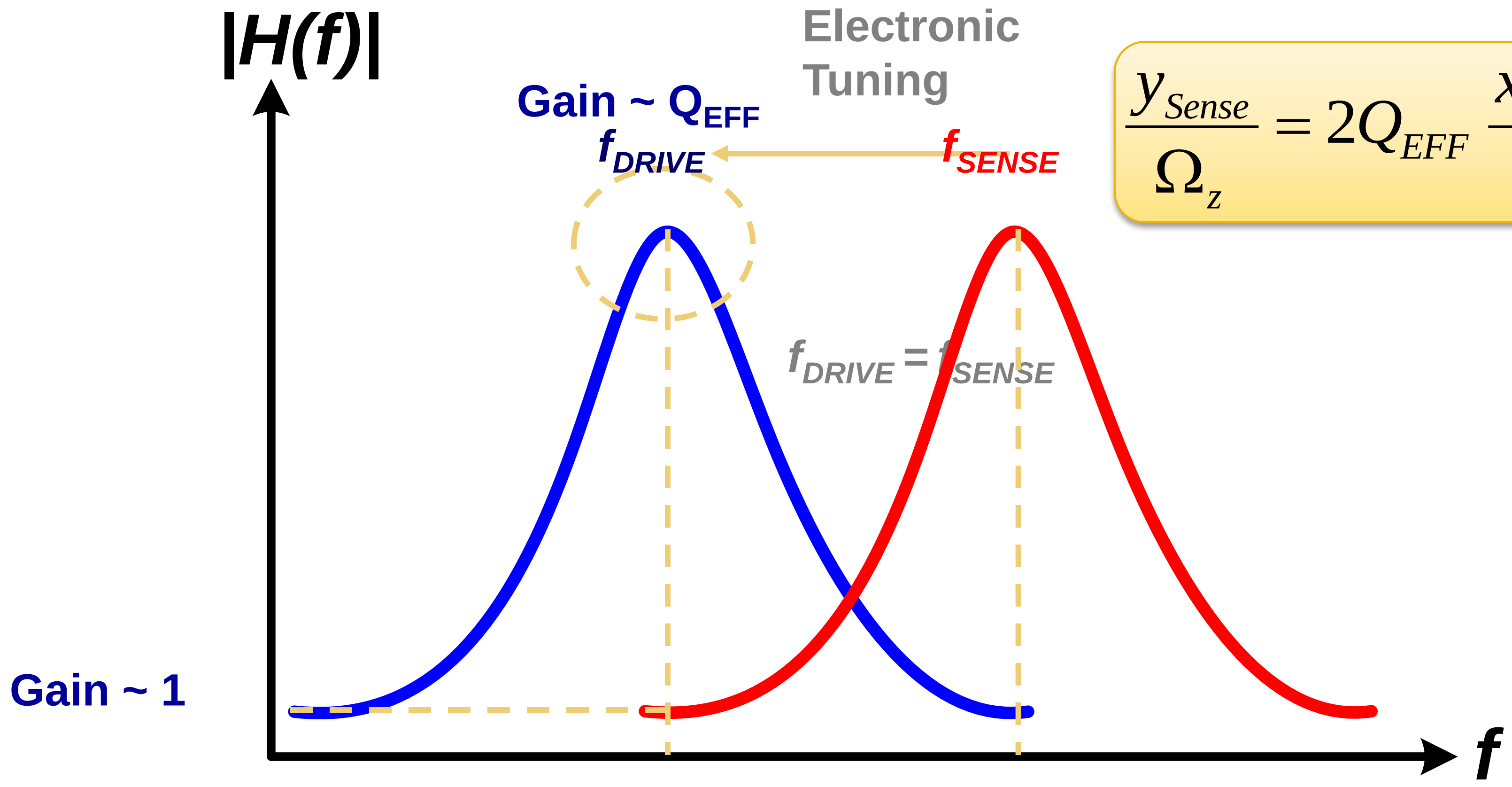

$$\frac{y_{Sense}}{\Omega_z} = 2Q_{EFF}\frac{x_{Drive}}{\omega_0}$$

Mode-Matching - Example

- Split is reduced from 45Hz down to 0Hz on a tuning-fork gyroscope

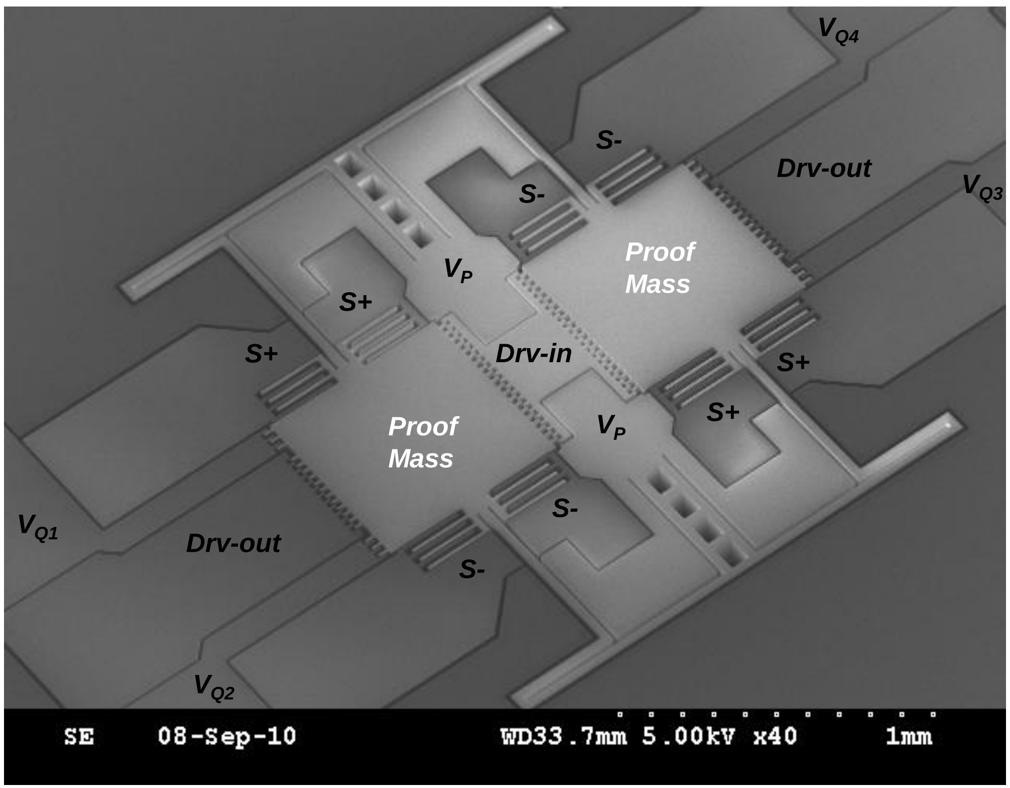

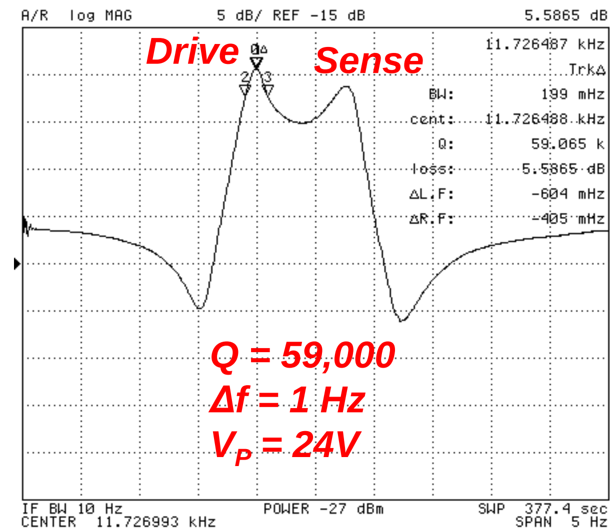

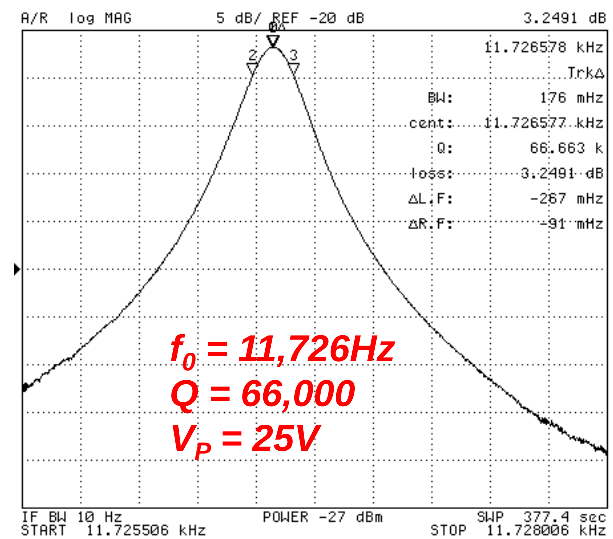

Georgia Tech

Current Sensing Topologies

Switched-Capacitor Integrator

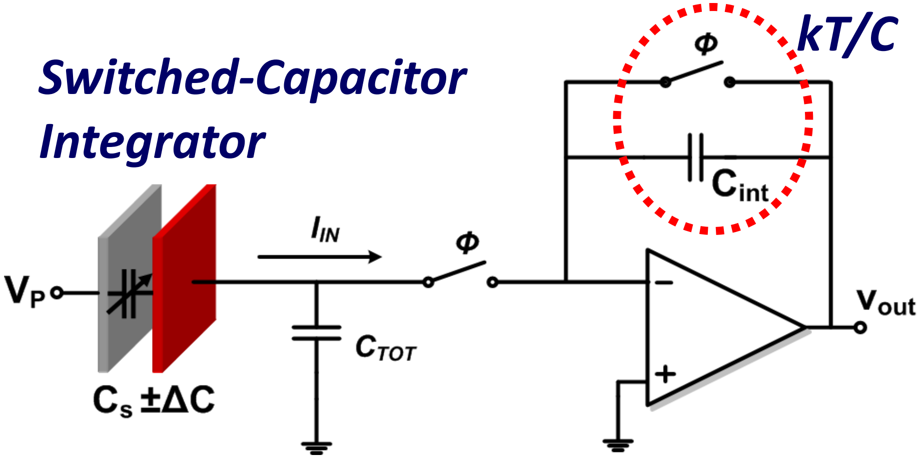

Continuous-Time Source-Follower

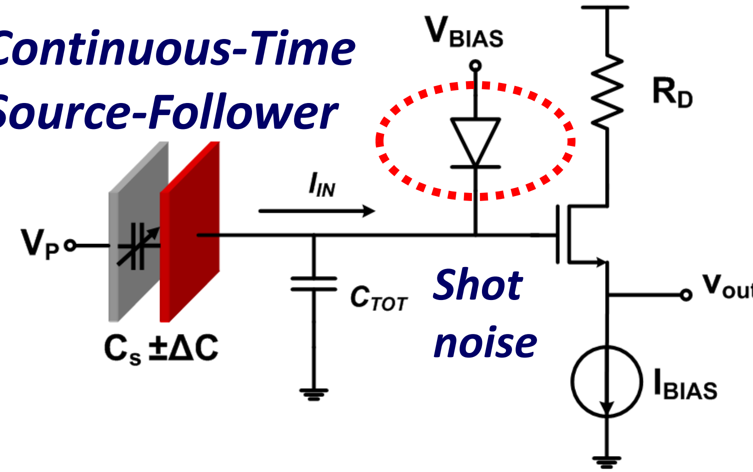

Continuous-Time Charge-Integrator

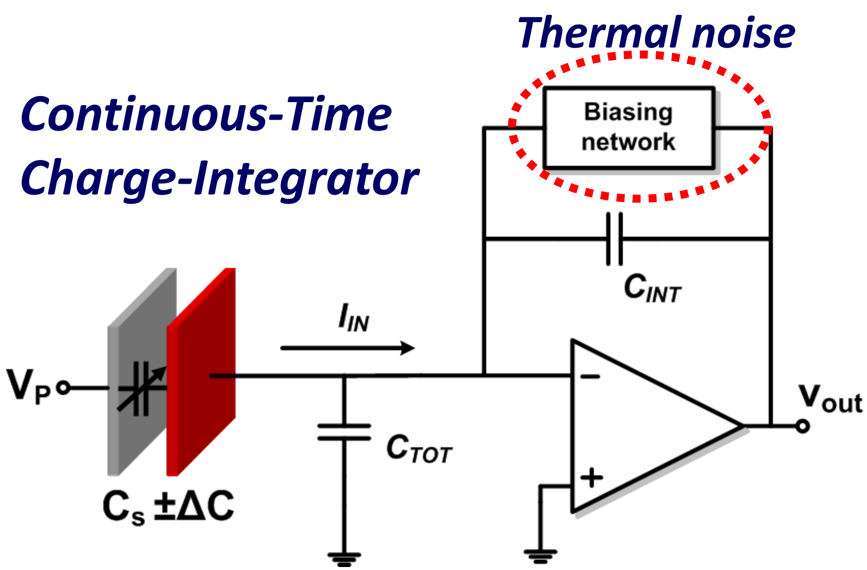

Transimpedance Amplifier (TIA)

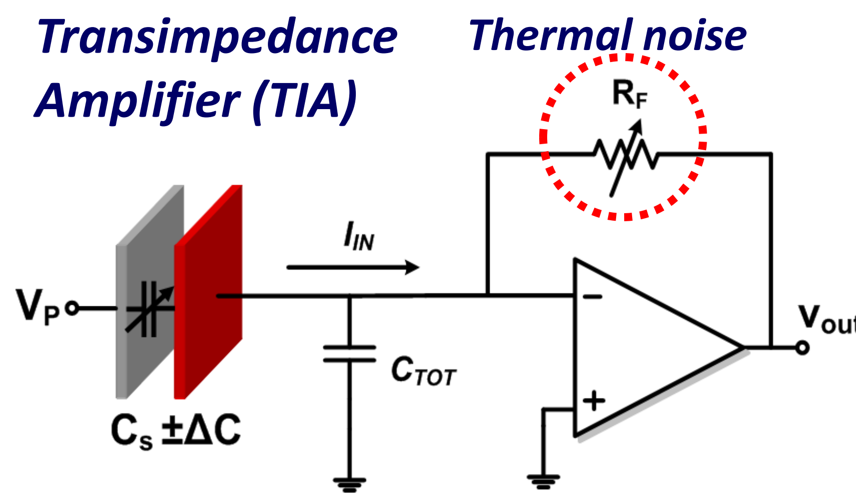

Transimpedance Amplifier (TIA)

- Amplify sense current I_{Sense} into output voltage V_{out}:

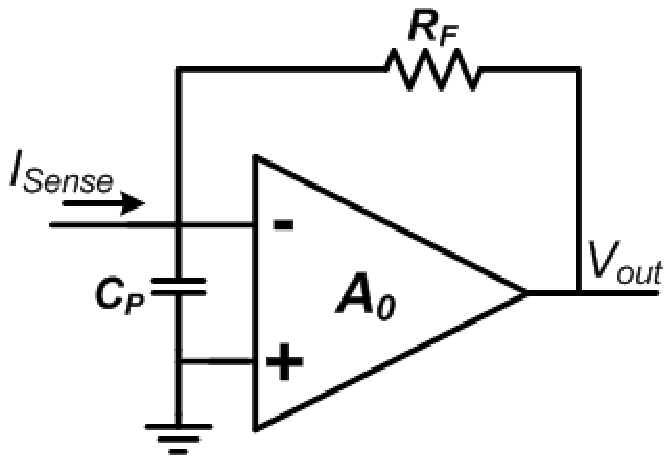

$$\frac{V_{out}}{I_{sense}} = \frac{R_F A_0}{1 + A_0}$$

$$R_{in,TIA} = \frac{R_F}{1 + A_0}$$

- Reduced input resistance:
  - High bandwidth
  - Minimum Q-loading on the resonator
- Reduced output resistance:
  - Good buffering for the subsequent amplifiers
- Bias adjusted by feedback
  - No need to bias network

MEMS Gyroscope Interface Architectures

- Amplitude demodulation:
  - Coherent demodulation of amplitude-modulated rate from Coriolis signal
  - Force-to-rebalance architecture
- Frequency demodulation:
  - Resonant output FM gyroscope
  - Quadrature FM (QFM) gyroscope
- Phase demodulation:
  - Phase-readout and self-calibration architecture

Coherent AM Readout

- Actuate the drive mode at resonance
    - demodulate rate from Coriolis output
- Drive loop uses an AGC loop for start-up and drive amplitude control
- TIA front-end used for minimal loading and optimum noise performance

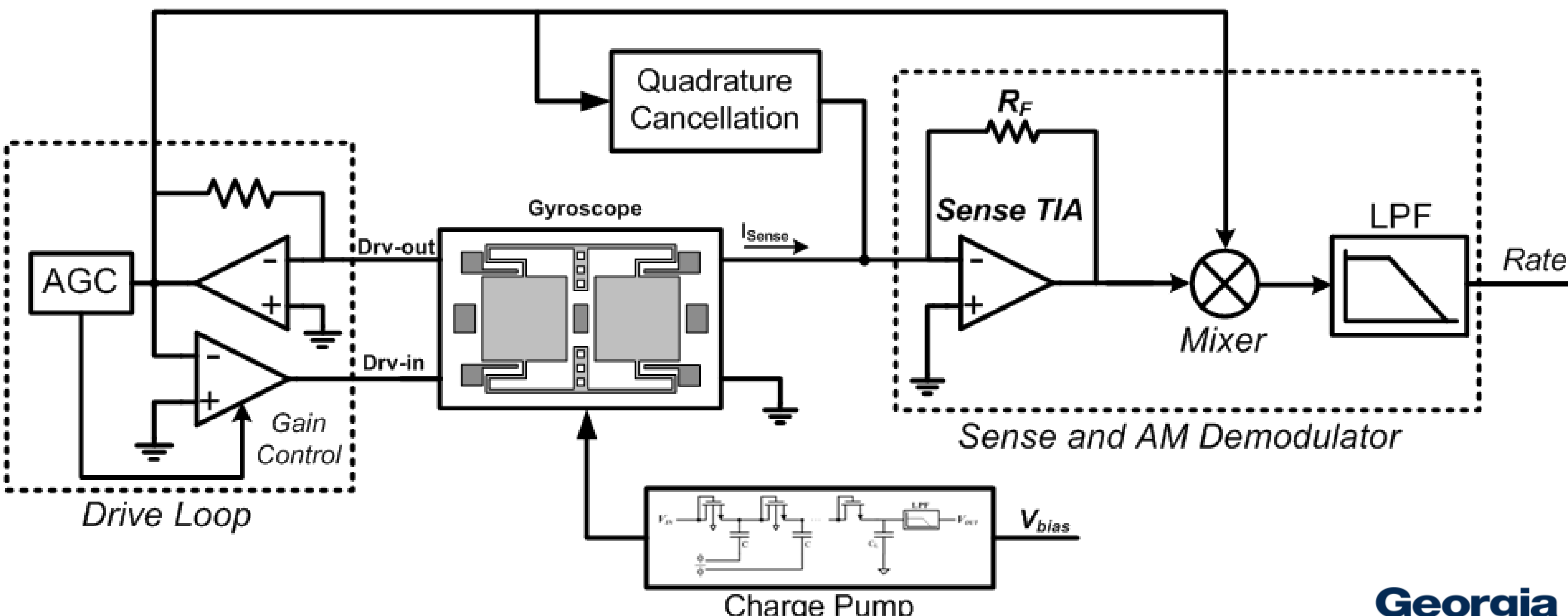

Coherent AM Readout – Drive Loop

- Barkhausen criteria provided by TIA-based drive-loop
- Automatic gain control (AGC) loop used to start-up oscillations and to stabilize v_{drive} amplitude
- PI controller is used to remove steady state error

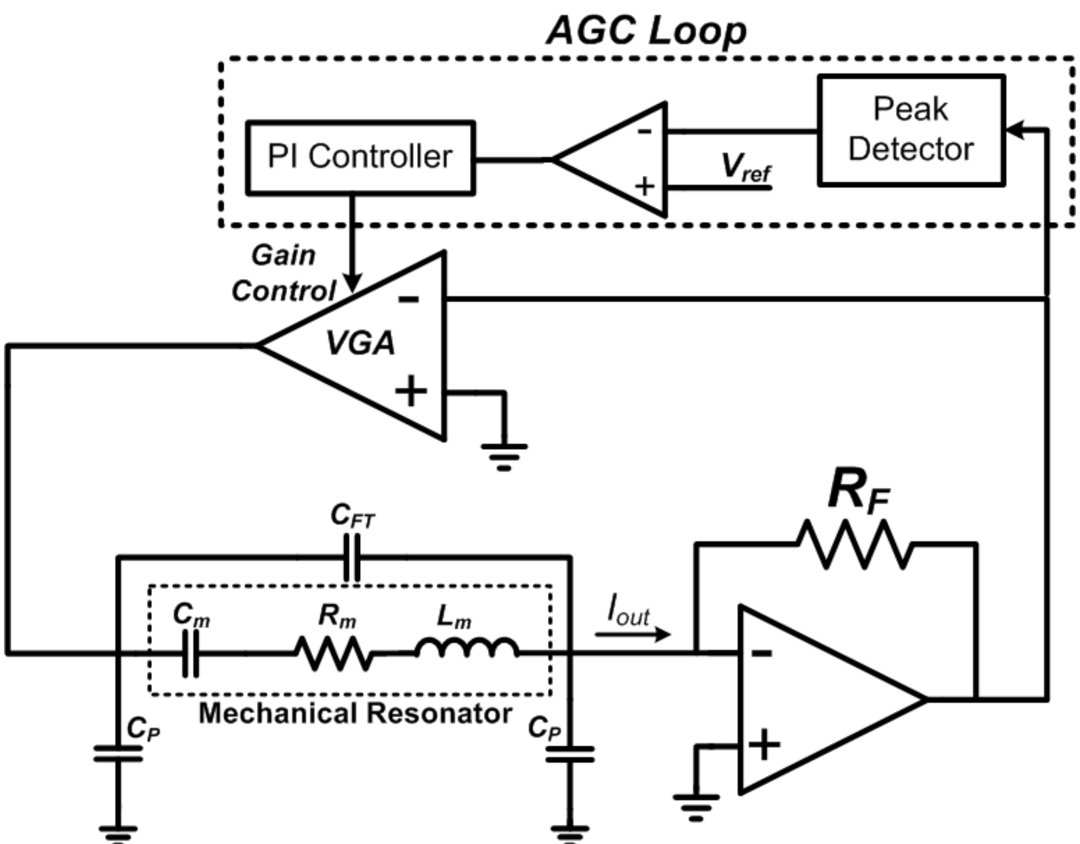

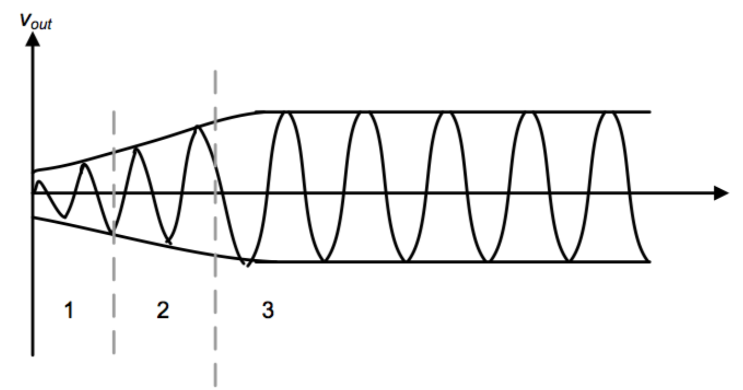

1. *Start-up region*
2. *Nonlinear transient region*
3. *Steady-state region*

Motional Resistance – Design Implications

- Output current of sensor:

$$I_{sensor} \propto \frac{V_P Q_{sense} x_{drive}}{d_{s0}} \Omega_z$$

- Implication of large motional resistance:
  - Larger drive voltage is needed
  - Large TIA gain
  - Higher power dissipation
  - Poor drive-loop phase noise

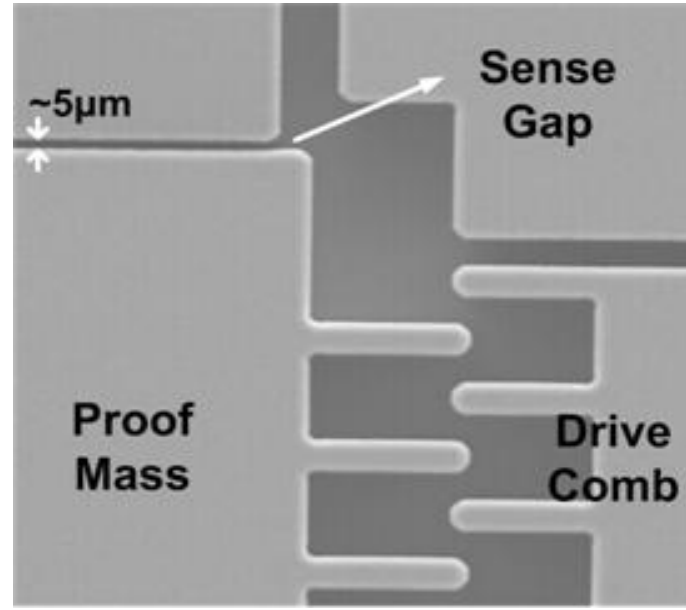

Close-up of sense gap and drive combs in a tuning-fork Gyroscope (TFG)

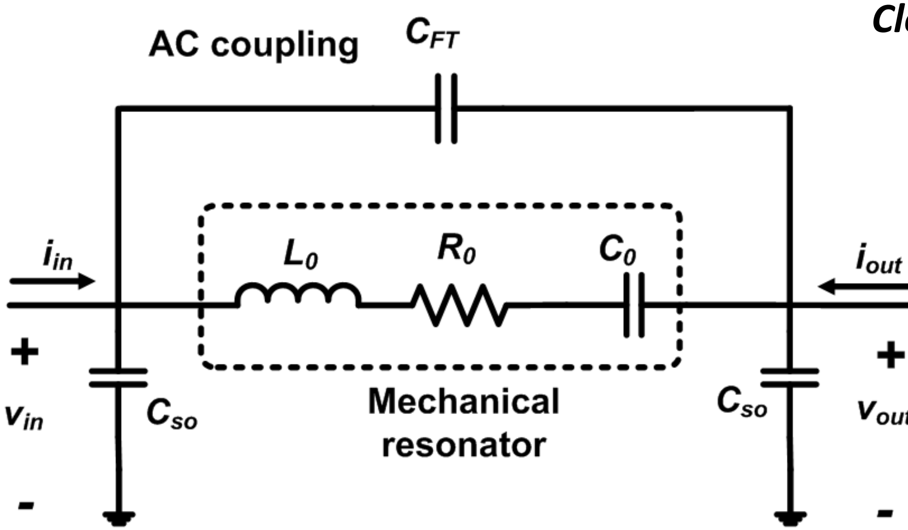

TIA Gain and Frequency Response

- In addition to the Opamp poles, ω_{p1} and ω_{p2}, the closed-loop TIA configuration adds an extra pole to the loop-gain transfer function:

$$LG(s) = \frac{A_0}{(1+s/\omega_{p1}).(1+s/\omega_{p2}).(1+R_F C_p s)}$$

$$\frac{V_{Sense}}{I_{Sense}} = \frac{R_F \times LG(s)}{1+LG(s)}$$

- TIA stability must be analyzed accounting for the additional pole caused by C_P.

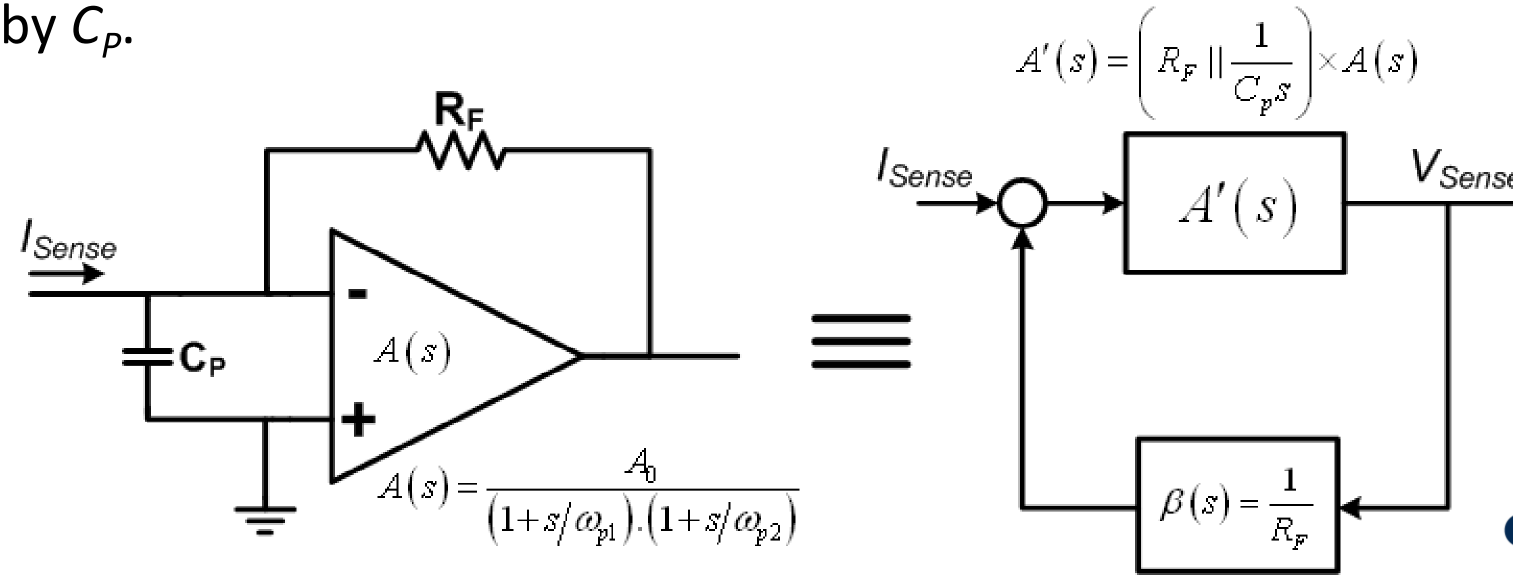

TIA Compensation

- Adding a miller feedback capacitor increases phase margin and improves stability by adding a zero:

$$LG(s) = \frac{A_0(1+R_F C_F s)}{(1+s/\omega_{p1}).(1+s/\omega_{p2}).(1+R_F(C_p+C_F)s)}$$

$$\frac{V_{Sense}}{I_{Sense}} = \frac{R_F \times LG(s)}{1+LG(s)}$$

- Large R_F provides better stability, yet larger phase shift in the amplified output:

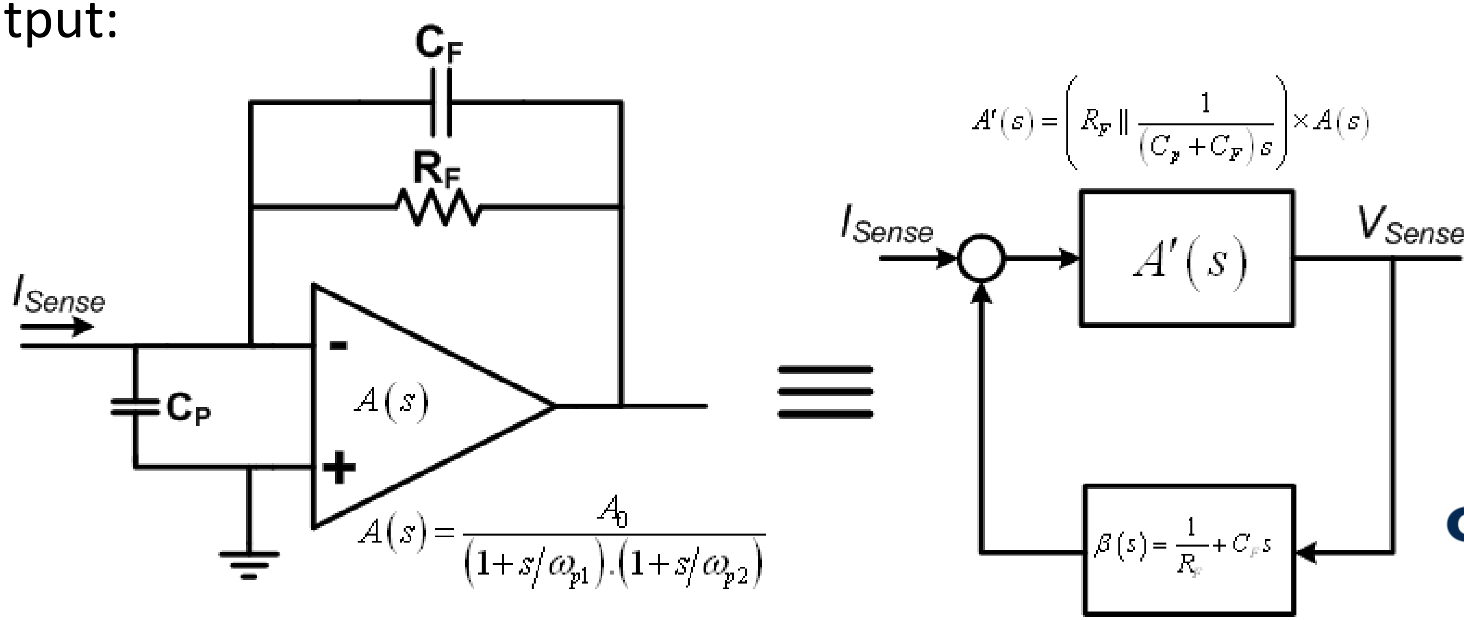

TIA Input-referred Current Noise

- Input-referred current noise of a TIA:

$$ENE\Omega = \frac{d_{s0}}{2V_P C_{s0} Q_{EFF} x_{drive}} . I_{n,tot} . \sqrt{BW}$$

$$\overline{i_{n,tot}^2} \approx \frac{4k_B T}{R_F} + \overline{v_{n,op}^2} \times \left(\frac{1}{R_F^2} + \omega^2 C_{tot,in}^2 \right)$$

- Above a certain value of R_F, the input-referred noise is dominated by R_F noise only.
  - Larger R_F → Lower current noise

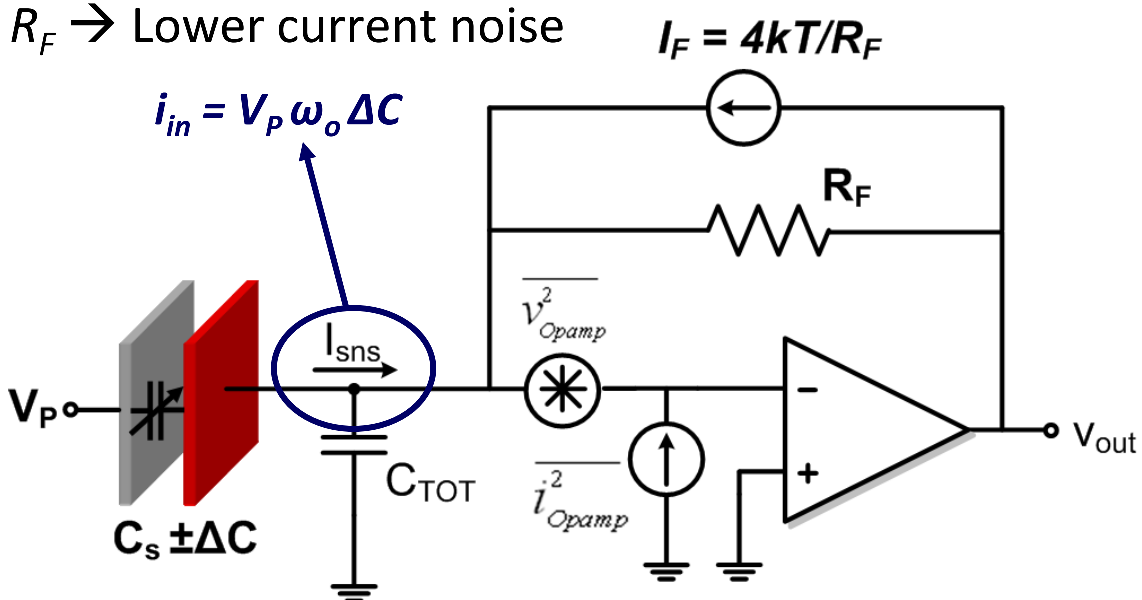

Drive Loop – Capacitive Feedthrough

- Anti-resonance is a result of feedthrough (C_{FT}) and pad capacitances (C_p)
- Locking into parallel resonance due to drive-loop phase shifts
  - phase criteria is provided by high-Q resonator.
- Locking to a higher frequency where magnitude is higher and phase is 0°

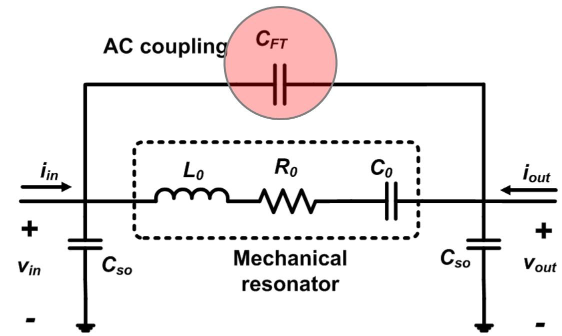

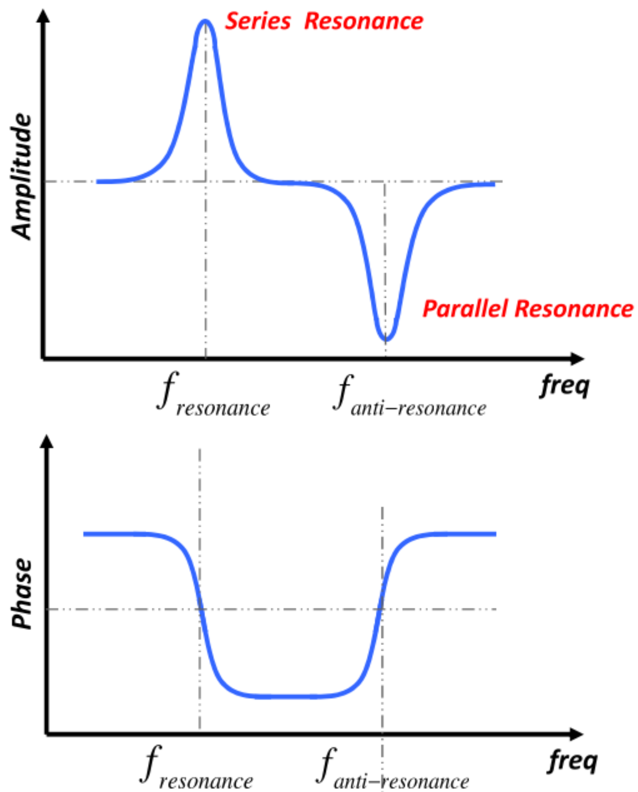

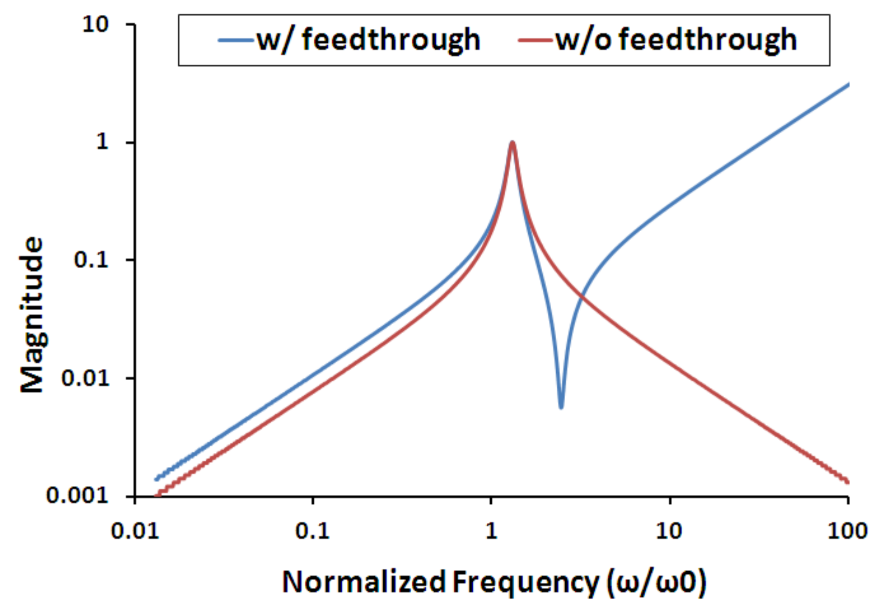

Georgia Tech

Drive Loop – Series Resonance

- Locking to series resonance needed to:
  - Maximize scale factor
  - Minimize quadrature error
- Analog/ Digital Phase shifting can compensate additional phase shift.

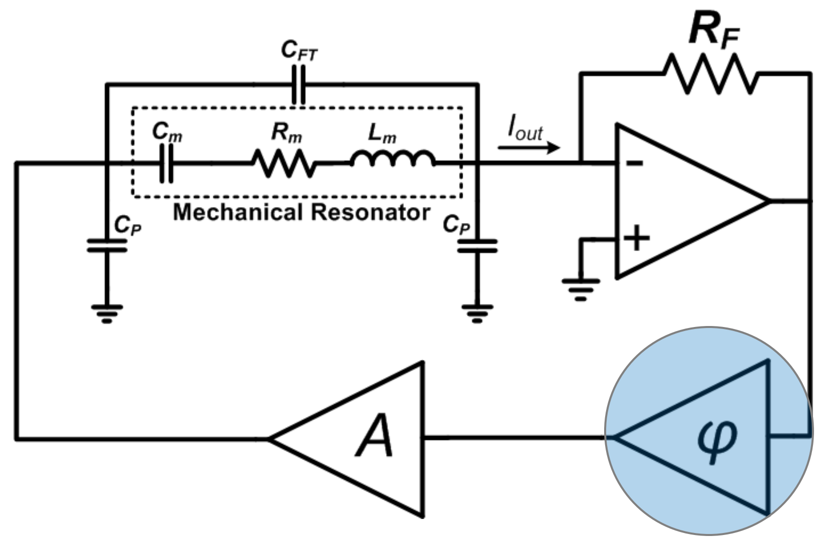

- All-pass analog shifters:

$$\frac{v_{out}}{v_{in}} = \frac{1 - R_{in}C_{in}s}{1 + R_{in}C_{in}s} = 1\measuredangle -2\tan^{-1}\left(R_{in}C_{in}\omega\right)$$

$$\frac{v_{out}}{v_{in}} = \frac{-1 + R_{in}C_{in}s}{1 + R_{in}C_{in}s} = 1\measuredangle \pi -2\tan^{-1}\left(R_{in}C_{in}\omega\right)$$

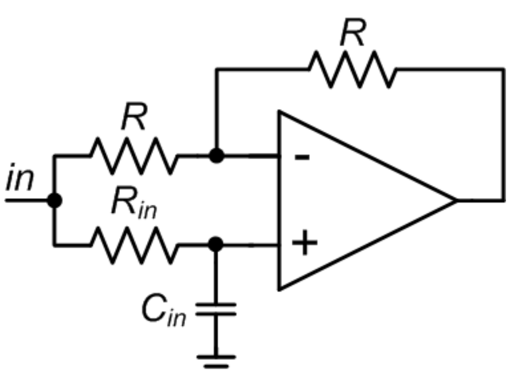

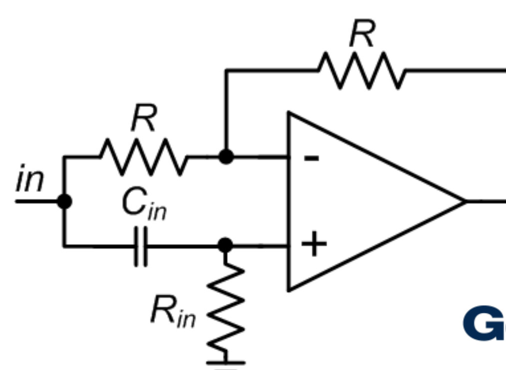

Drive Loop – Feedthrough Cancellation

- Locking to a higher frequency where magnitude is higher, and phase is 0°:
  - Extra low-pass filtering needed
  - Phase-shifter is needed
- Feedthrough cancellation circuit can eliminate the effect of C_{FT}:

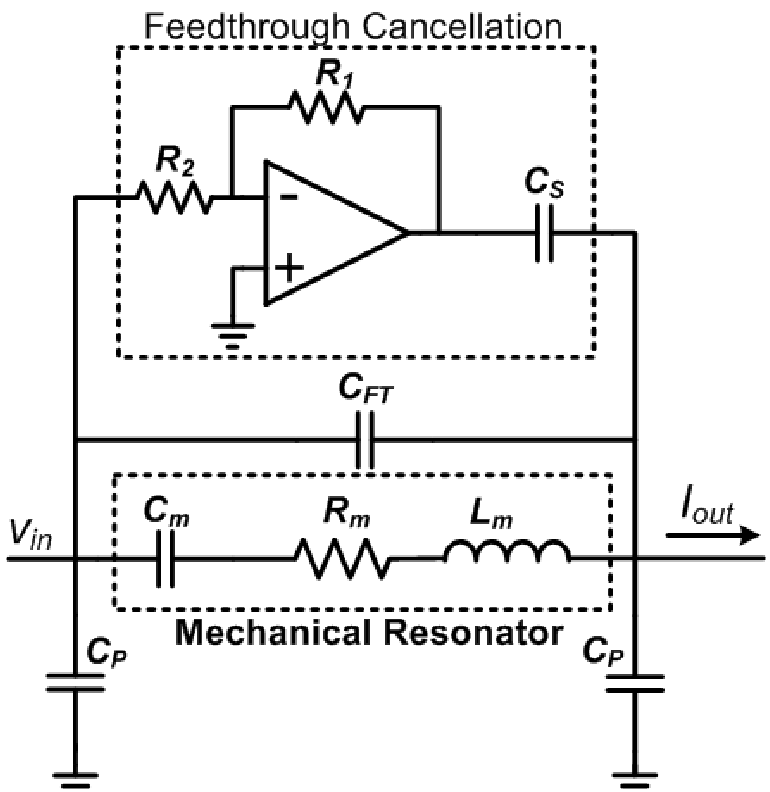

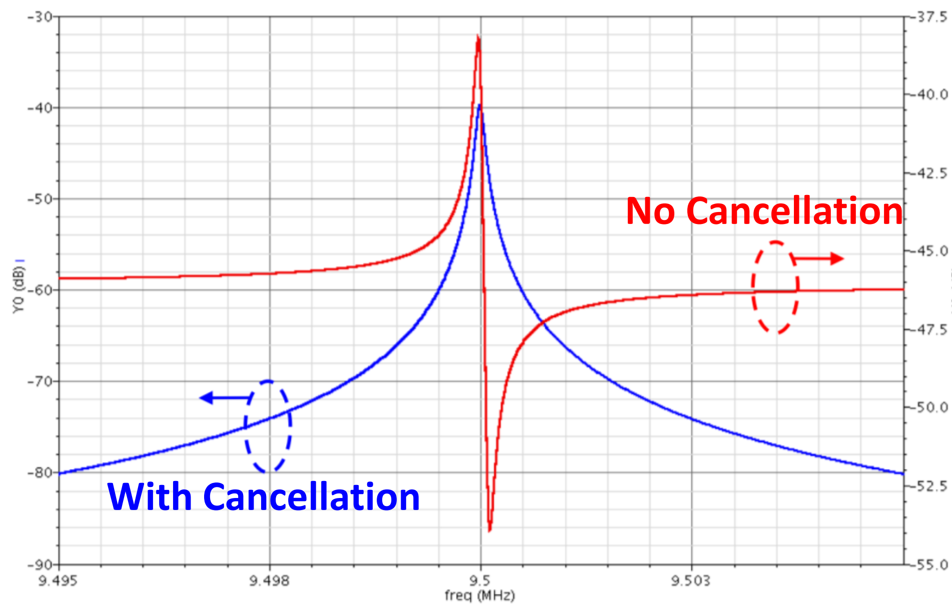

Sense TIA Front-end and Demodulator

- Sense TIA amplifies the sense current into sense voltage.
- AM rate is down-converted by multiplication of Coriolis output into drive signal.
- Phase-shifter is used in drive signal path to compensate the phase-shift induced by the sense front-end amplifiers and filters.

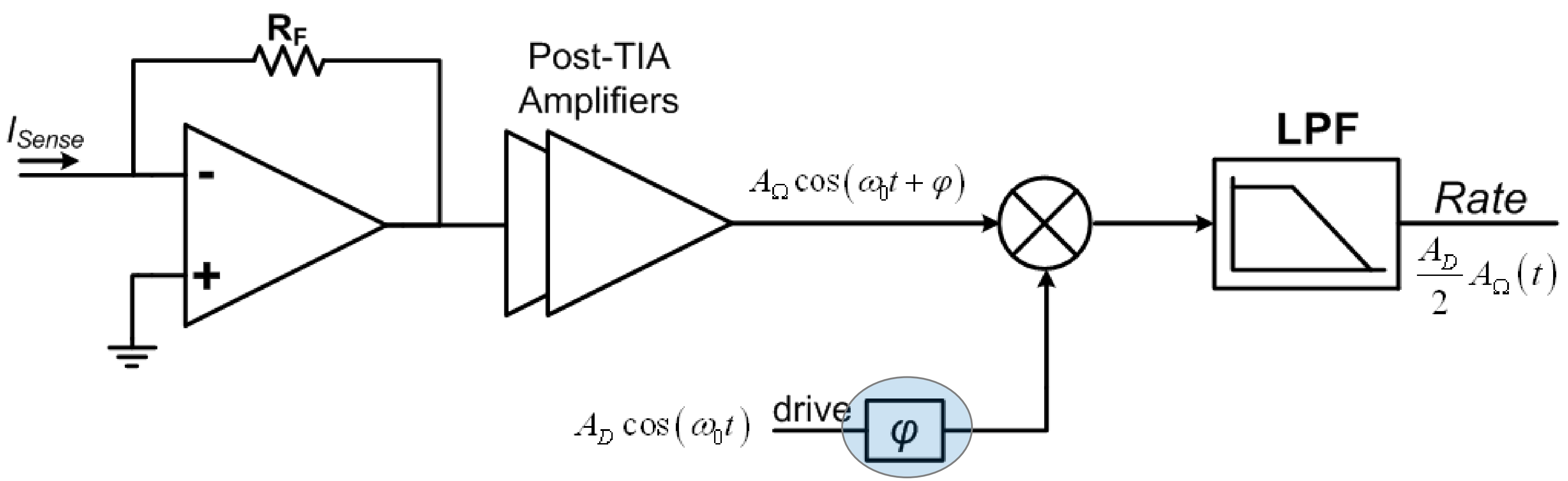

Effect of Quadrature

- Besides Coriolis signal, the gyroscope sense current has a quadrature component caused by misalignments and fabrication imperfections:

$$\left.\begin{array}{l} Coriolis \propto velocity \\ ZRO \propto displacement \end{array}\right\} \Rightarrow 90^\circ \; phase\,difference$$

$$f_{Drv} = f_{sns} \Rightarrow v_{drive} = A_D \cos \omega_0 t \Rightarrow \begin{cases} i_{Coriolis} = A_\Omega \cos \omega_0 t \\ i_{Quad} = A_Q \sin \omega_0 t \end{cases}, A_Q \gg A_\Omega$$

- Coherent AM demodulation eliminates quadrature phase data from rate output, however:
  - Accurate phase adjustment is required in the demodulator drive path to compensate for sense front-end phase-shift
  - Quadrature is typically 2-3 orders of magnitude larger than Coriolis full-scale
  - Large quadrature saturates TIA output → TIA gain must be reduced
    → degrades SNR and Dynamic Range
  - Feedthroughs and other error sources can change the ZRO phase.

Error Sources and Noise Analysis

- **Bias drift:** Random variation in the bias (ZRO) over time – long-term drift
- **Sense front-end noise →** thermal and flicker
    - Minimum detectable rate:

$$TNE\Omega = \sqrt{MNE\Omega^2 + ENE\Omega^2}$$

$$MNE\Omega \propto \frac{1}{x_{drive}} \sqrt{\frac{4k_B T}{\omega_0 M Q_{EFF}}},\ ENE\Omega \propto \frac{d_{s0}}{V_P C_{s0} Q_{EFF} x_{drive}} . I_{N-total}$$

- **drive-loop phase noise:**

$$v_{drive} = A_D \cos\left(\omega_0 t + \varphi_n(t)\right), \begin{cases} i_{Coriolis} = A_\Omega \cos\omega_0 t \\ i_{Quad} = A_Q \sin\omega_0 t \end{cases},\ \varphi_n(t) \ll 1$$

$$\Rightarrow \begin{cases} rate = \dfrac{A_D . A_\Omega}{2} \cos\left(\varphi_n(t)\right) \approx \dfrac{A_D . A_\Omega}{2}\left(1 - \varphi_n^2(t)\right) \\ offset = -\dfrac{A_D . A_Q}{2} \sin\left(\varphi_n(t)\right) \approx -\dfrac{A_D . A_Q}{2} \varphi_n(t) \end{cases}$$

→ *Negligible effect on rate*

→ *Low-frequency bias noise*

Georgia Tech

Charge Pump

- Required to generate large, on-chip DC polarization voltages for gyroscope
  - Typically a cascade of voltage-doubler stages
  - High voltage generation – may need 20V or higher depending on device
  - No current consumption – electrostatic polarization of capacitive MEMS
  - Resistive loading – significantly reduces maximum pump V_{out}
  - Parasitic capacitors act as voltage dividers, reducing maximum V_{out}
  - Clock frequency practically limited to less than a few hundred kHz
    - » Ripple reduction, losses through stray capacitances
  - Body effect – increase in V_{SB} after each pump stage makes V_t larger and reduces the subsequent pump gain

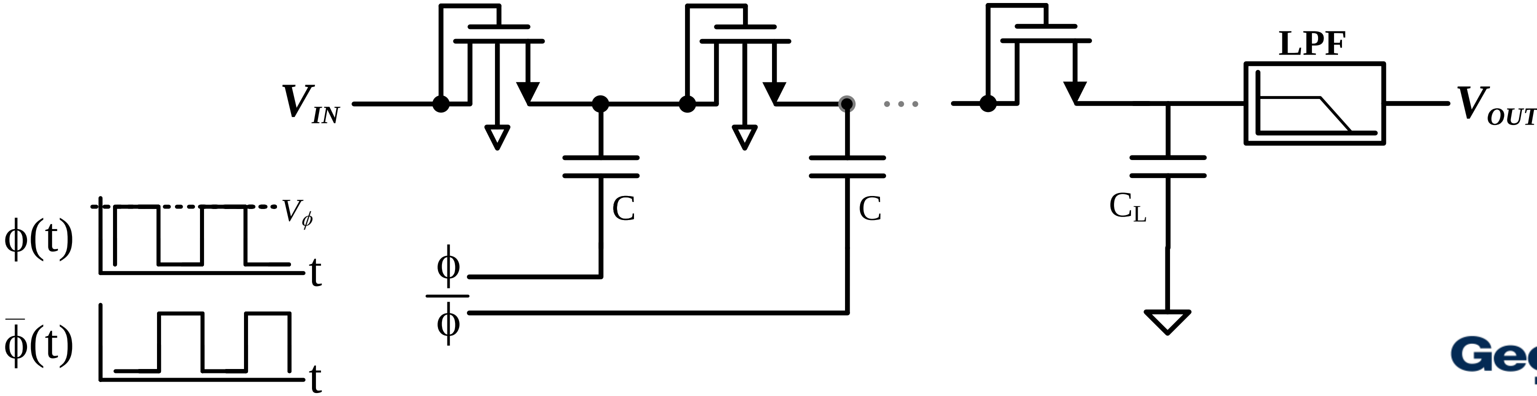

STM Gyroscope Interface ASIC (1)

- Drive loop:
  - SC charge amplifier used for current sensing
  - SC band-pass filter used to remove residual offset and phase-adjustments
  - Output of 2nd order Chebyshev LPF is regulated using a PI-controller AGC loop
  - PLL is used to generate all the timing for SC blocks

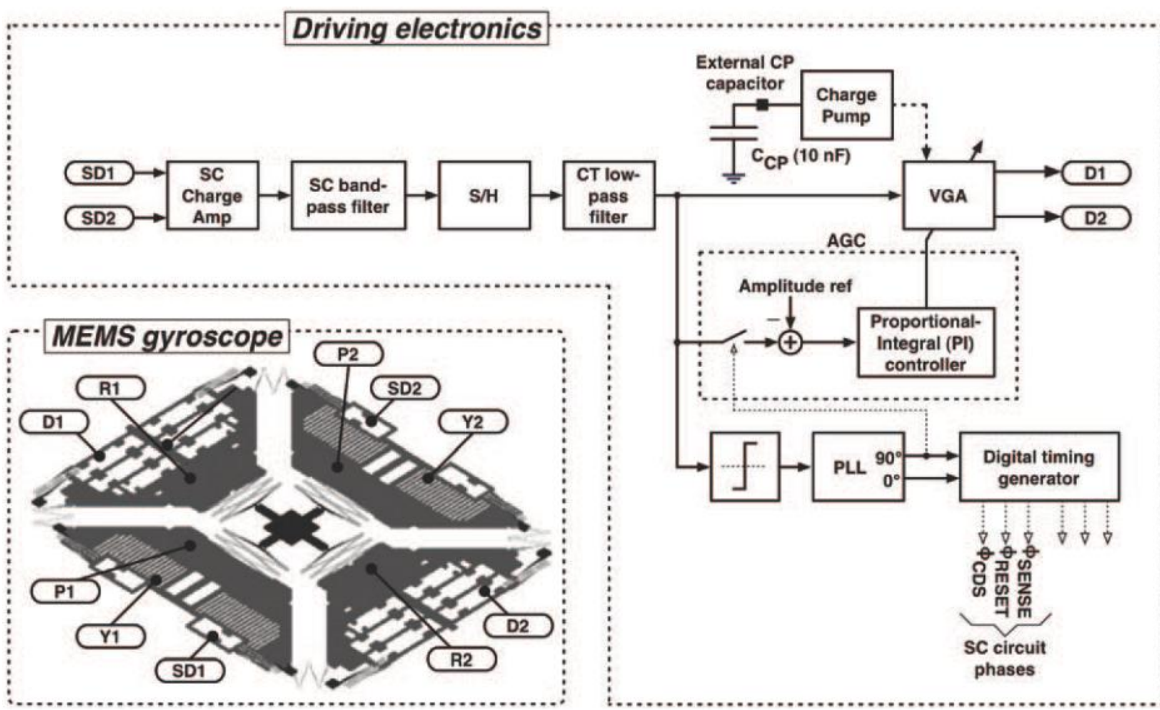

[Prandi et al, ISSCC 2011]

STM Gyroscope Interface ASIC (2)

- Sense chain:
  - Time-division multiplexed open-loop readout interface
  - Charge amplifier is used for current sensing
  - Demodulation carrier in-phase with the drive mode velocity
  - SC low-pass filtering
  - 12-bit SAR ADCs used to provide digital output from three gyroscope axes
  - Temperature compensation done on the digital output

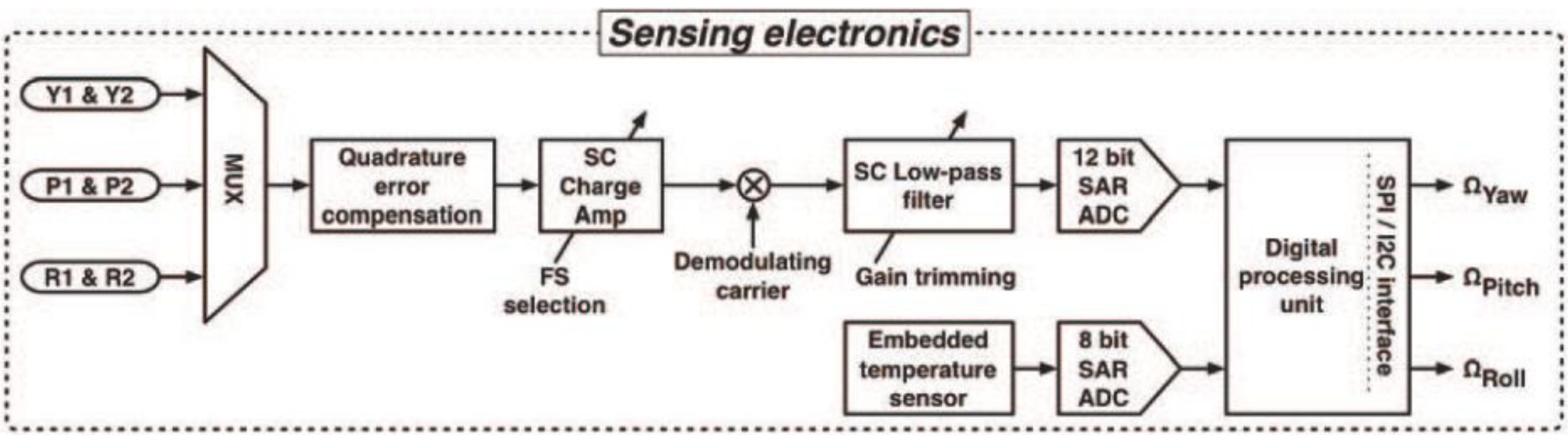

[Prandi et al, ISSCC 2011]

Georgia Tech

Invensense Gyroscope Interface ASIC

- Sense chain:
  - Charge amplifier is used for current sensing
  - Programmable capacitors used for transcap amplifiers
  - Amplitude control block regulates drive-mode displacement
  - Gain and offset trimming performed on digital output rate

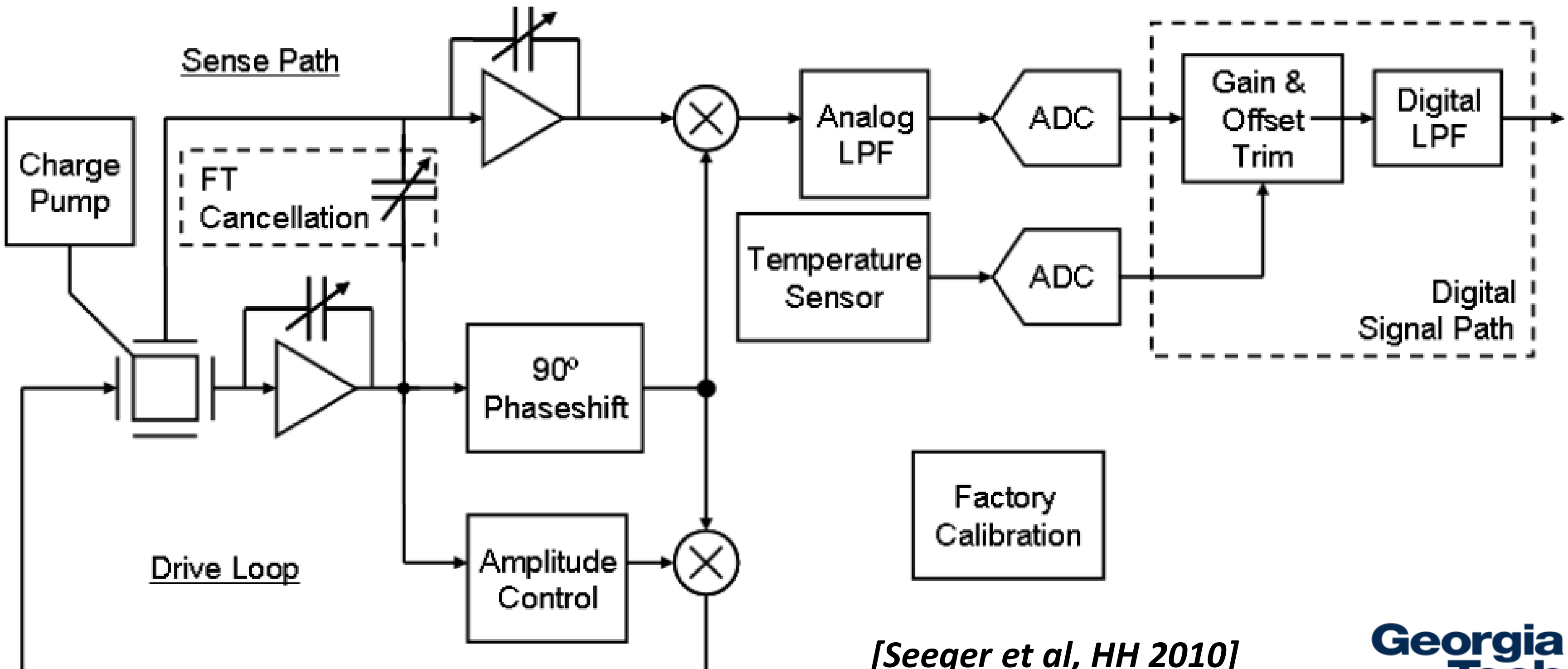

[Seeger et al, HH 2010]

Georgia Tech

Force-to-Rebalance Architecture

- Drive loop used to actuate the drive mode of the sensor
- Feedback provides the force needed to rebalance sense displacement
    - Sense displacement is maintained at zero
- Enhance bandwidth for mode-matched gyroscopes
- Provide digital ΣΔ output
- Use sensor element as loop filter for additional noise-shaping

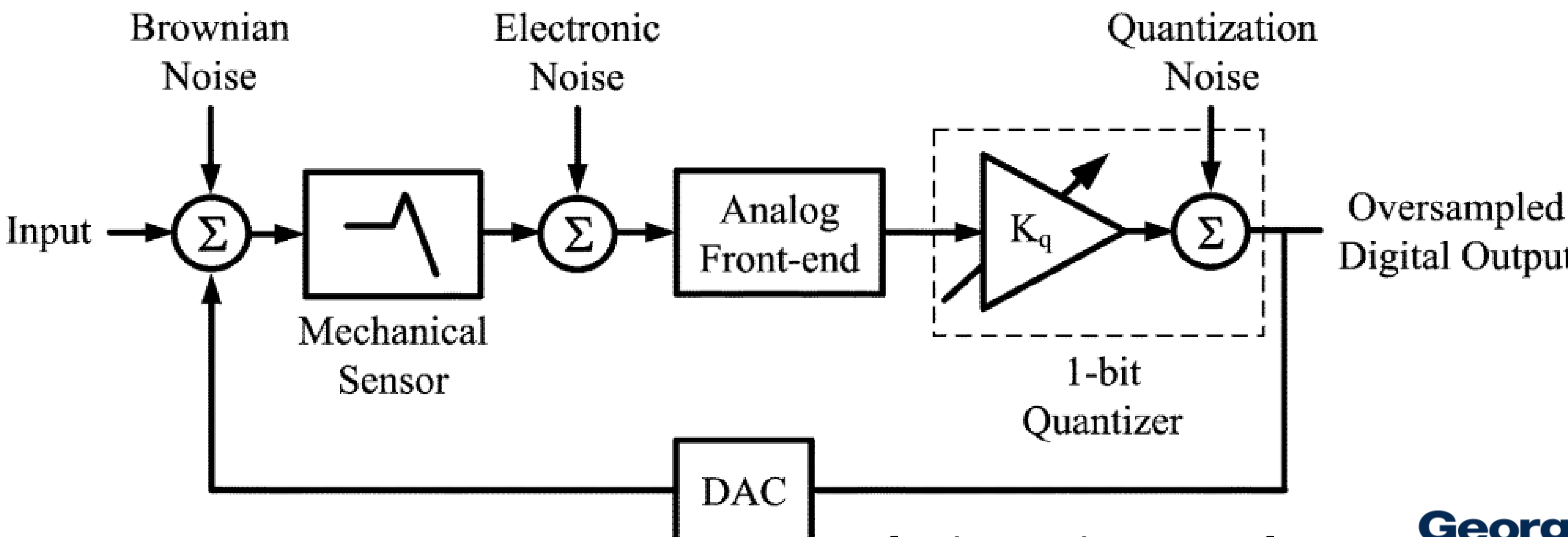

[Petkov et al, JSSC 2005]

Georgia Tech

FM Gyroscope

- Periodic compression and tension of the tuning-fork tines by Coriolis force at the proof-mass drive frequency modulates the resonant frequency of the force sensors.
- Displacement is both AM and FM modulated.
- Differential sensing can improve sensitivity to temperature and pressure.
- Oscillator electronics noise can become the primary electronic noise source.

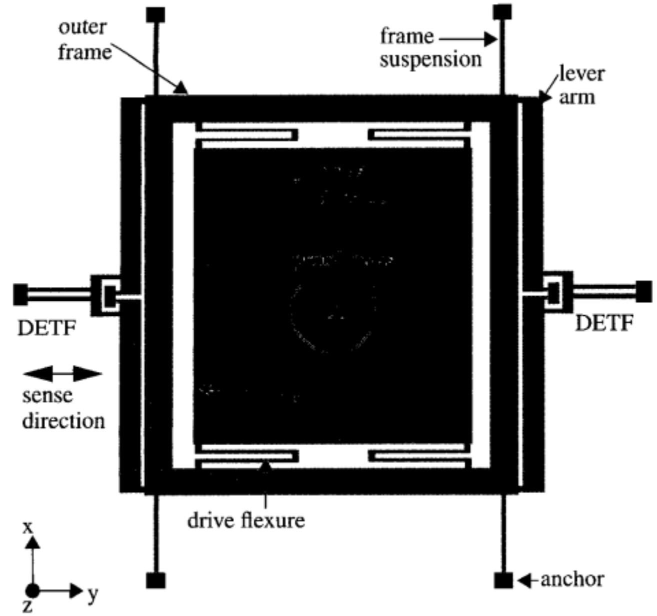

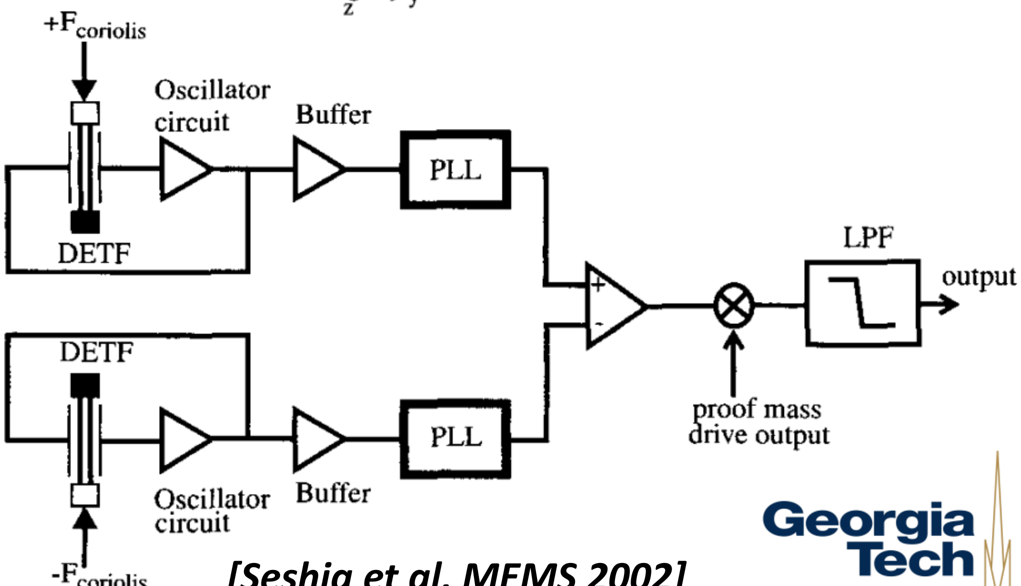

[Seshia et al, MEMS 2002]

Digitization Schemes

- ΣΔ ADC:
  the best match to digitize the low-frequency signal of the gyroscope
  - High SNR provided by oversampling and quantization noise shaping
  - >16 bits of resolution achieved easily
- ΣΔ force-to-rebalance

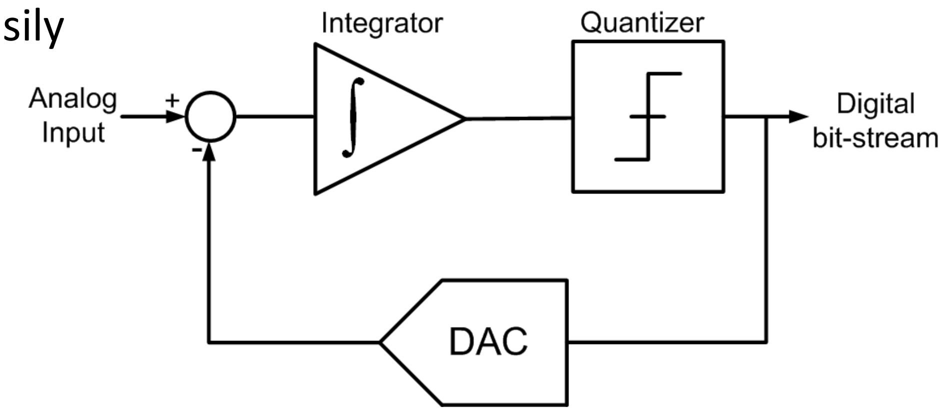

- SAR ADC:
  - Provide low-noise operation
  - Low-power consumption
  - Linearity limited to capacitance mismatch
  - Up to 12 bits of resolution

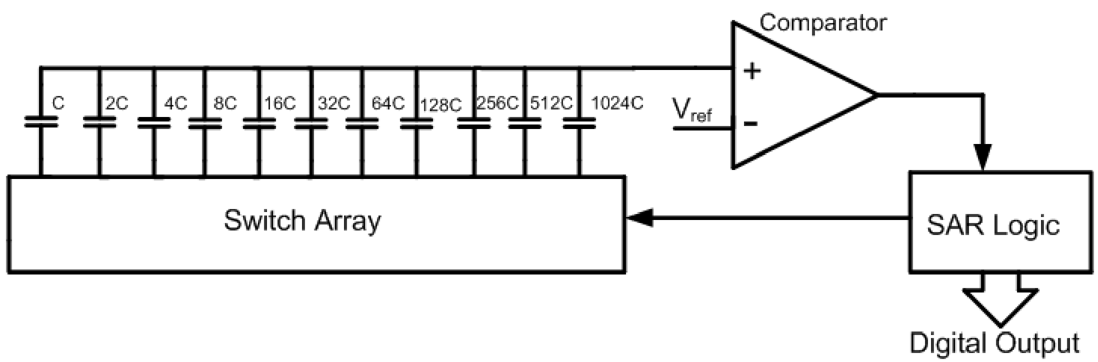

Georgia Tech

Frequency and Phase Demodulation for Gyroscope Self-Calibration

Self-Calibration Platform

- Calibrate scale factor and bias of the sensor frequently:
  - Compensate for long-term drifts in bias and scale factor of the mechanical part
  - Eliminate factory calibration
- Mechanical approach:
  - Rotary stage: hard to implement, needs very high accuracy
- Electrical approach:
  - QFM gyroscope: provide self-calibrated rate output
  - Phase-readout technique: provide electrostatic stimulus to mimic rotation

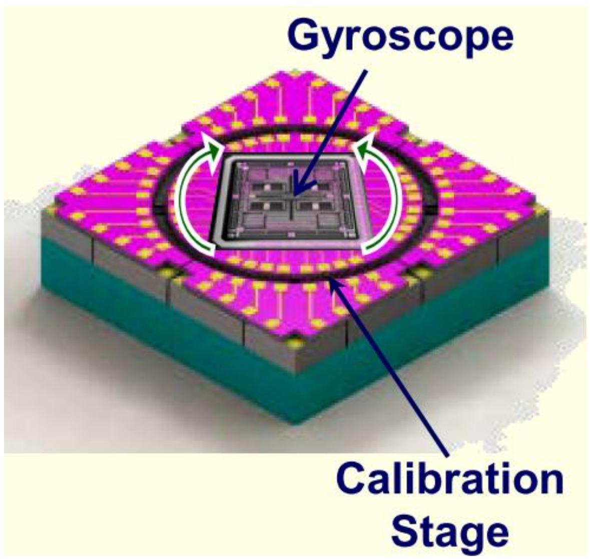

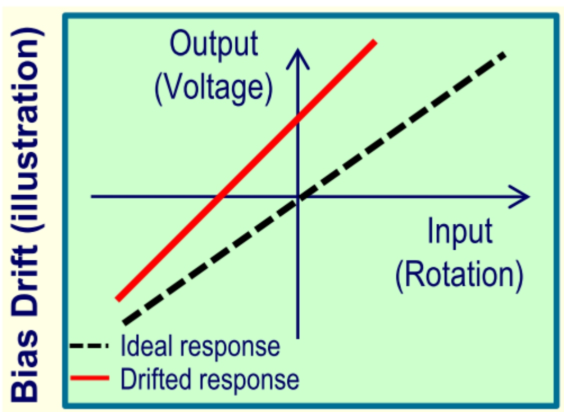

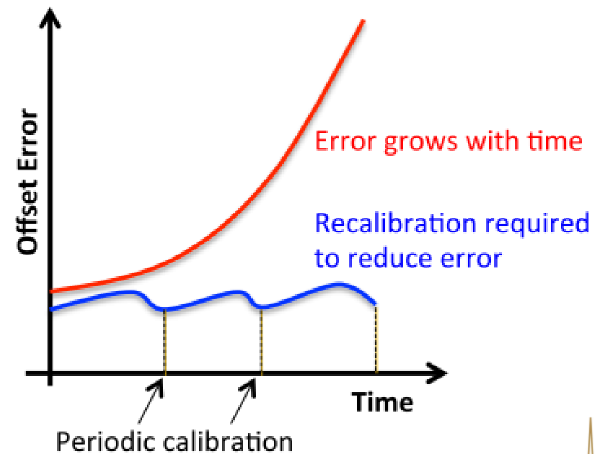

[Courtesy of Dr. Andrei Shkel, DARPA MTO]

Georgia Tech

Quadrature FM (QFM) Gyroscope

- Foucault pendulum gyroscope in QFM mode:
    - Outside observer perceives a frequency change of the gyroscope if he rotates relative to the sensor.
- Relies on nominally symmetric gyroscope design
- Scale factor independent of quality factor and electromechanical coupling factor.
- $\Delta\omega$ is independent of temperature, pressure, bias voltages, and fabrication imperfections.
- ω_s still drifts with temperature.

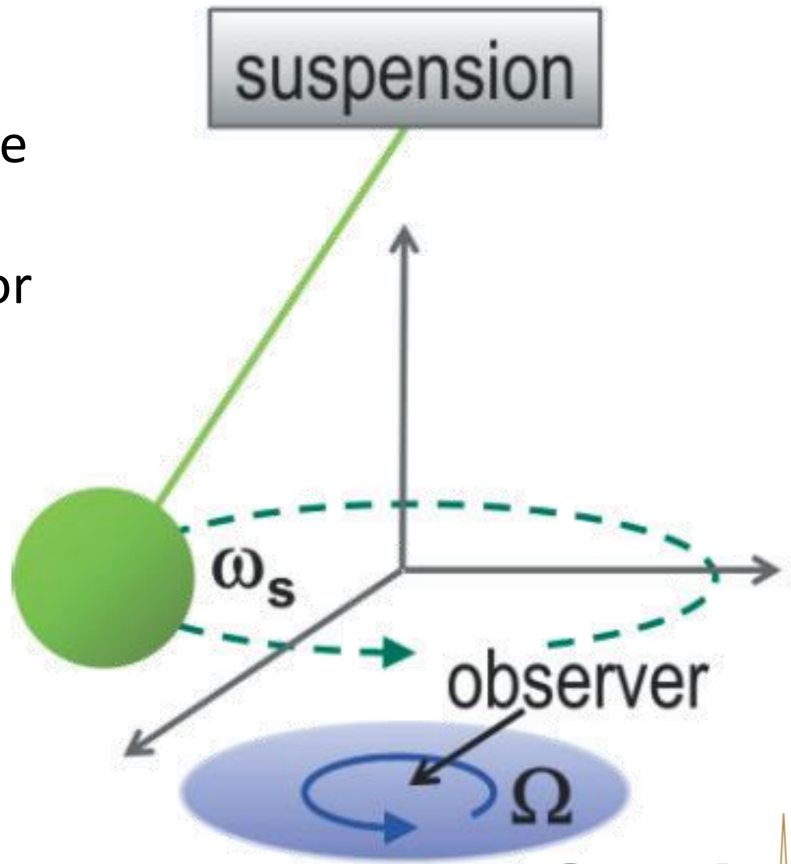

[Kline et al, MEMS 2013]

Georgia Tech

QFM Readout Architecture

- x and y oscillations controlled to equal amplitude and quadrature phase
- Circular actuation of the gyroscope modes to mimic the Foucault pendulum gyroscope
    - Frequency shift of the loops is measured as rate
- Real-time mode-matching is trivial
- Temperature, pressure and other environmental factors can produce false rate.

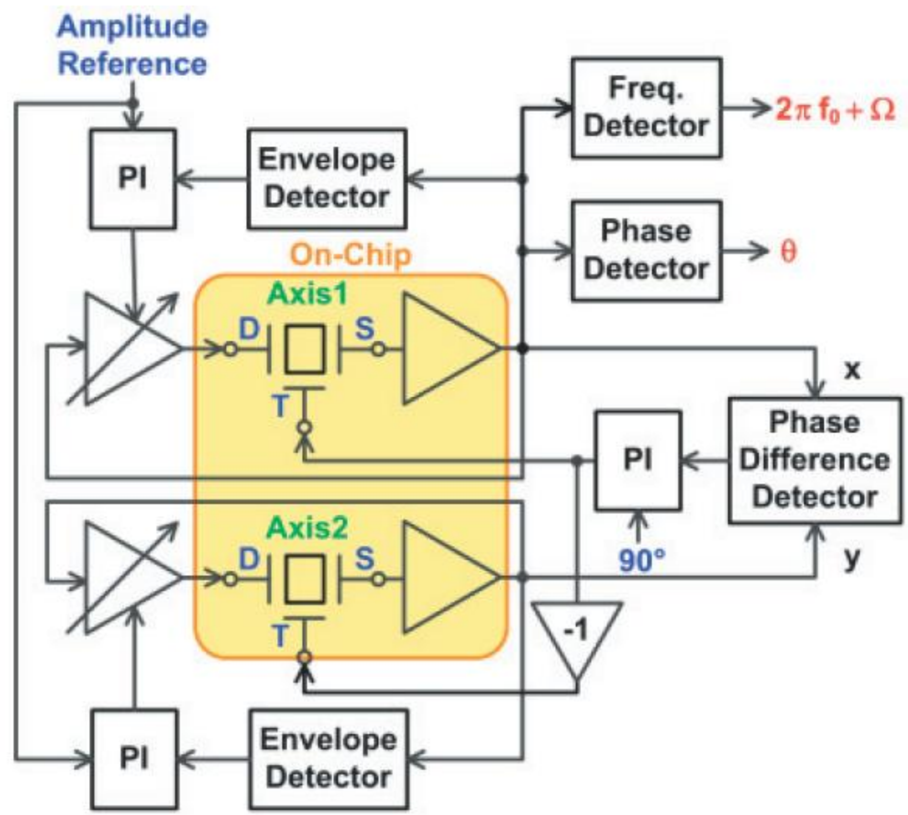

[Kline et al, MEMS 2013]

Georgia Tech

Dual-Mass Readout Architecture

- The gyro frequencies exhibit equal and opposite sensitivities to rate.
- The relative phase of the two oscillations is the integral of the frequency difference → output is a direct measure of the whole angle
- Temperature is common-mode in the differential sensing scheme
- Mismatch between two QFM gyros can introduce new error sources

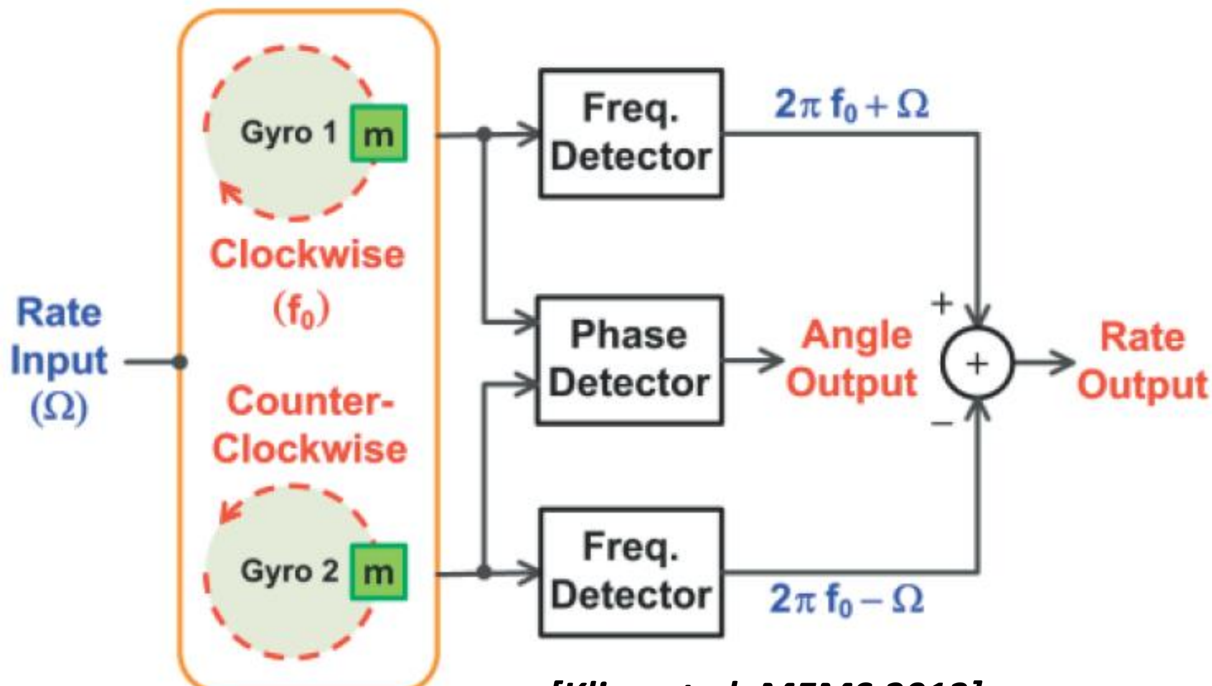

[Kline et al, MEMS 2013]

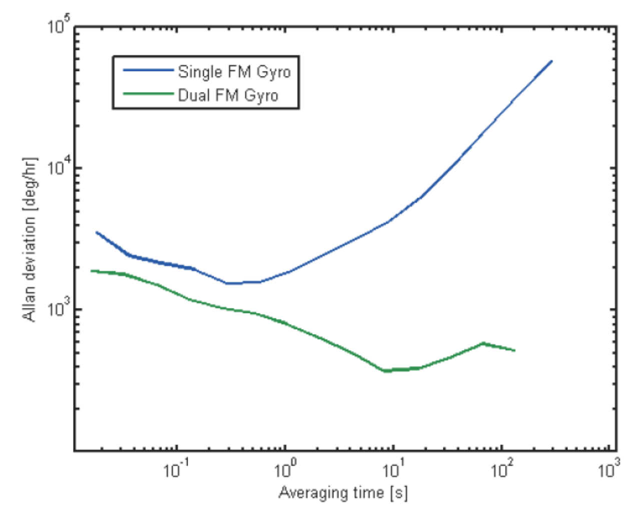

Improved Rate Random Walk (RRW)
RRW is attributed to environmental variations.

Georgia Tech

Phase-Readout and Self-Calibration

- Phase-readout architecture based on phase-shift induced in the gyro response due to rotation (Phase Modulation)
- Same concept can be utilized for self-calibration, using AM excitation.

Phase-readout:

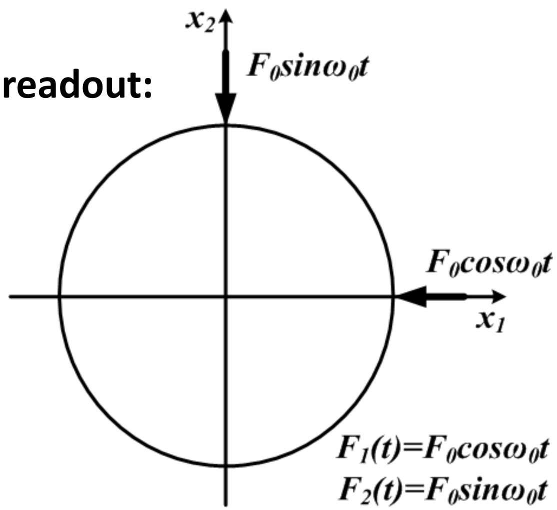

Calibration:

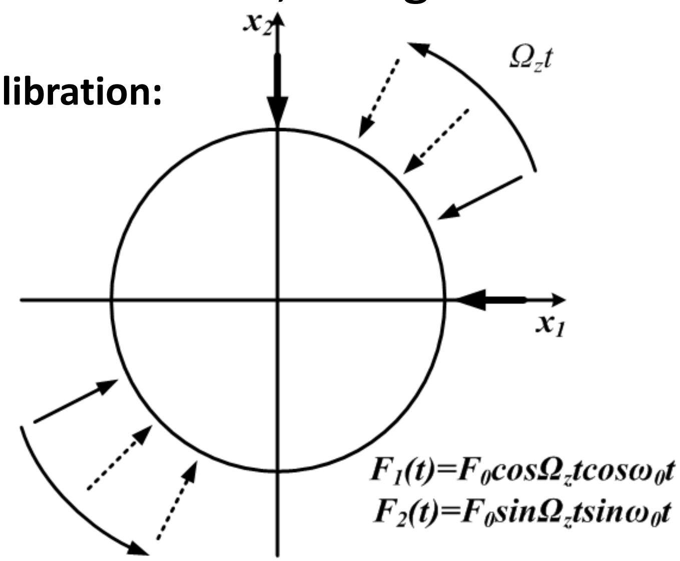

λ : Angular gain

$$\begin{cases} x_1(t) = A_1 \sin(\omega_0 t - \theta_0) \\ x_2(t) = A_2 \cos(\omega_0 t - \theta_0) \end{cases}$$

$$\theta_0 \cong \frac{2Q\lambda\Omega_z}{\omega_0}$$

$$\begin{cases} x_1(t) = (F_1/A)\cos(\Omega_z t - \theta_0)\sin\omega_0 t \\ x_2(t) = (F_2/A)\sin(\Omega_z t - \theta_0)\cos\omega_0 t \end{cases}$$

$$\theta_0 \cong \frac{2Q\Omega_z}{\omega_0}$$

[Casinovi et al, MEMS 2012]

Phase-Readout Architecture

- The Coriolis force creates a phase shift in the gyro outputs with respect to the inputs
- The phase shift is detected by synchronous phase demodulation.

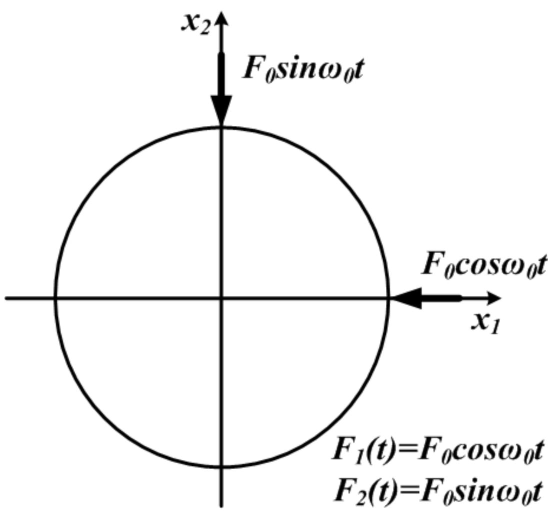

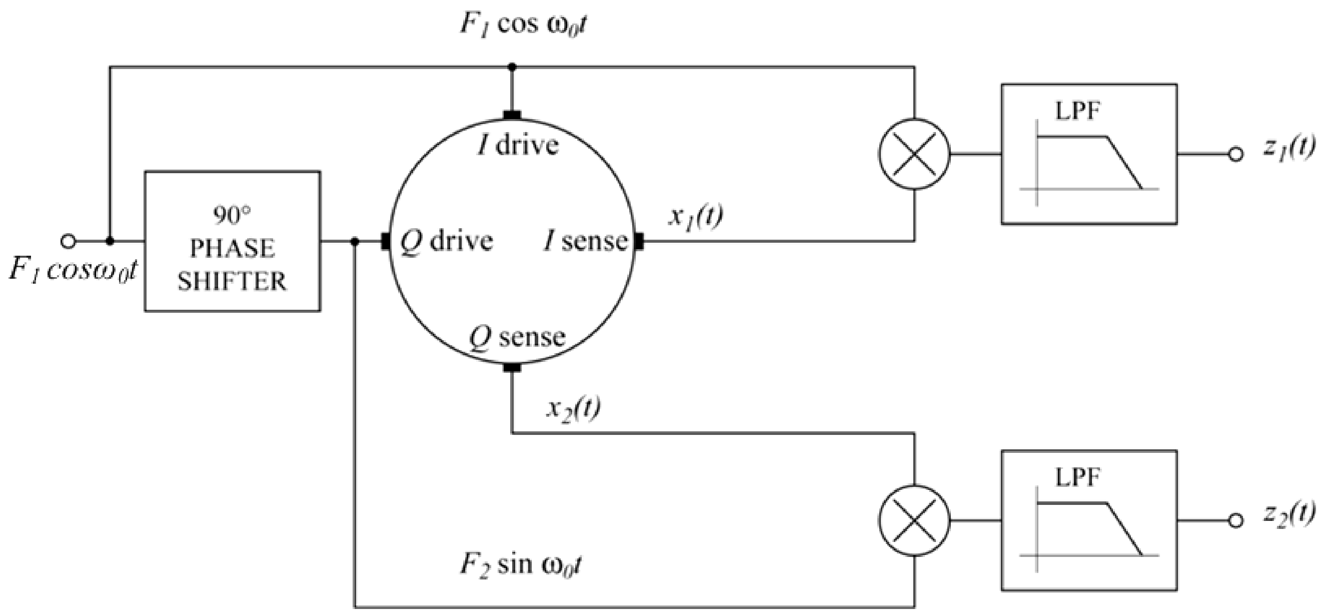

$$z_1 = z_2 = -\frac{F_1F_2}{\omega_0}\frac{\lambda\Omega_z}{(\omega_0/Q)^2 + (2\lambda\Omega_z)^2}$$

Self-Calibration Architecture

- Input excitations AM-modulated by quadrature-phase sinusoidal signals at angular frequency Ω_z
- Rotating excitation mimics mechanical rotation at Ω_z.

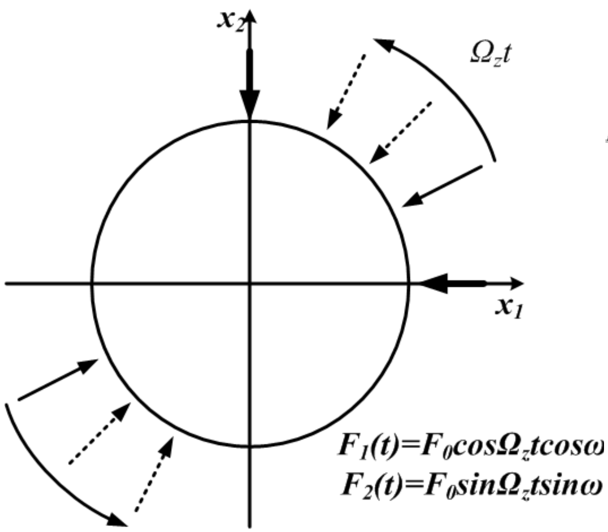

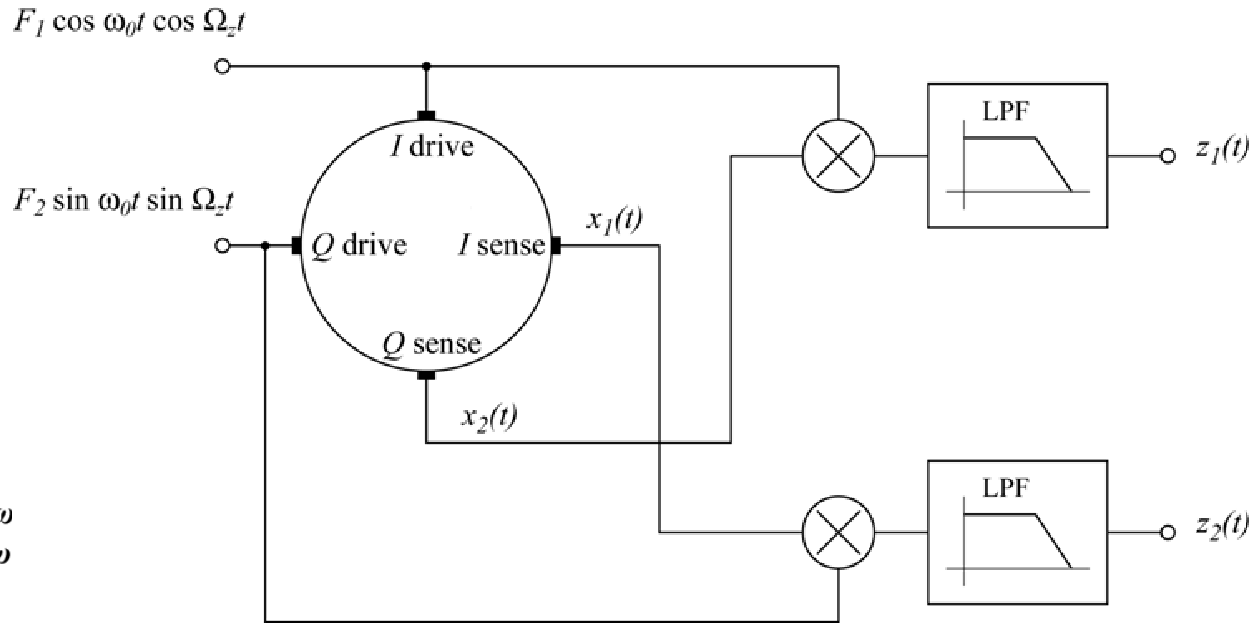

$$z_1 = z_2 = \frac{F_1 F_2}{2\omega_0} \frac{\Omega_z}{(\omega_0/Q)^2 + (2\Omega_z)^2}$$

Combined Readout and Self-Calibration

- Common electronics in both readout and calibration configurations
- Errors and drifts due to electronics will affect both modes equally

Readout Mode : $SELECT = 0; A(t) = DC$

$$\Rightarrow \begin{cases} F_1(t) = F_1 \cos \omega_0 t \\ F_2(t) = F_2 \sin \omega_0 t \end{cases}$$

Calibration Mode : $SELECT = 1; A(t) = \cos \Omega_Z t$

$$\Rightarrow \begin{cases} F_1(t) = F_1 \cos \Omega_Z t \cos \omega_0 t \\ F_2(t) = F_2 \sin \Omega_Z t \sin \omega_0 t \end{cases}$$

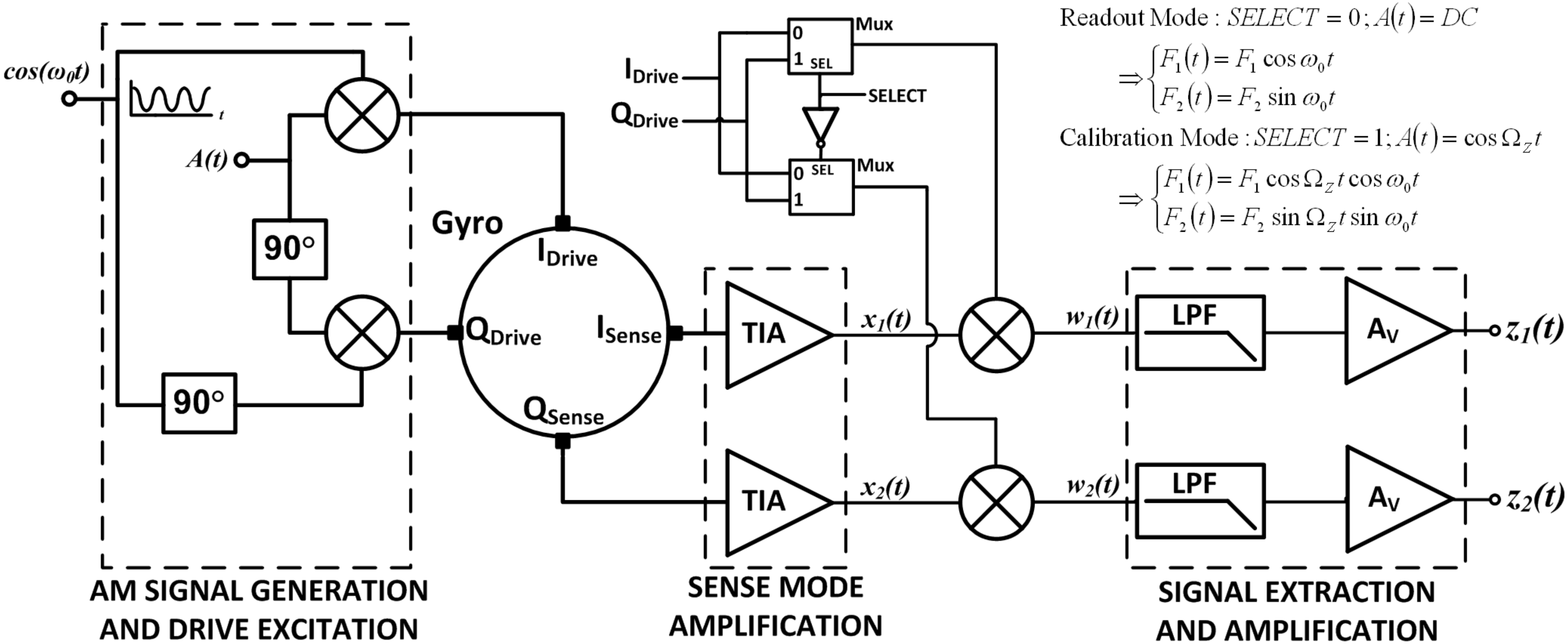

[N-Shirazi et al, Transducers 2013]

Georgia Tech

Calibration vs. Physical Rotation

- Calibration scale factor shows agreement with physical rate scale factor

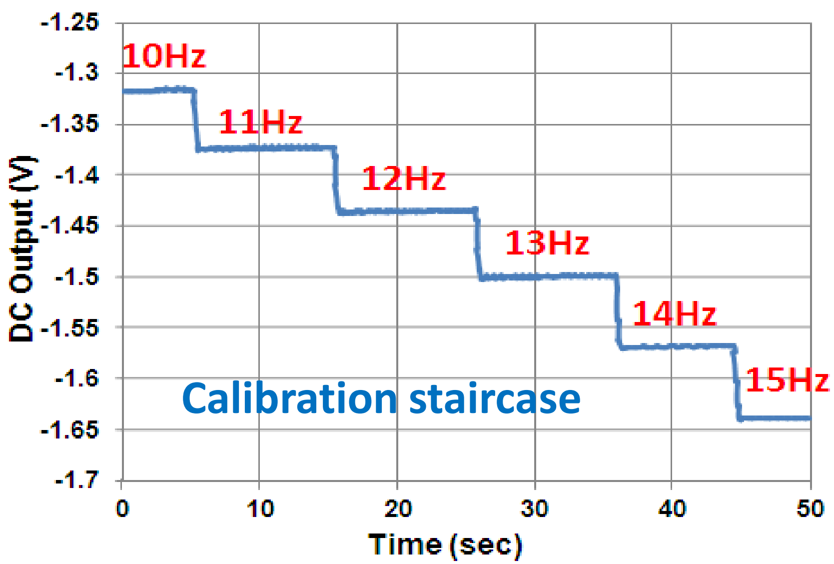

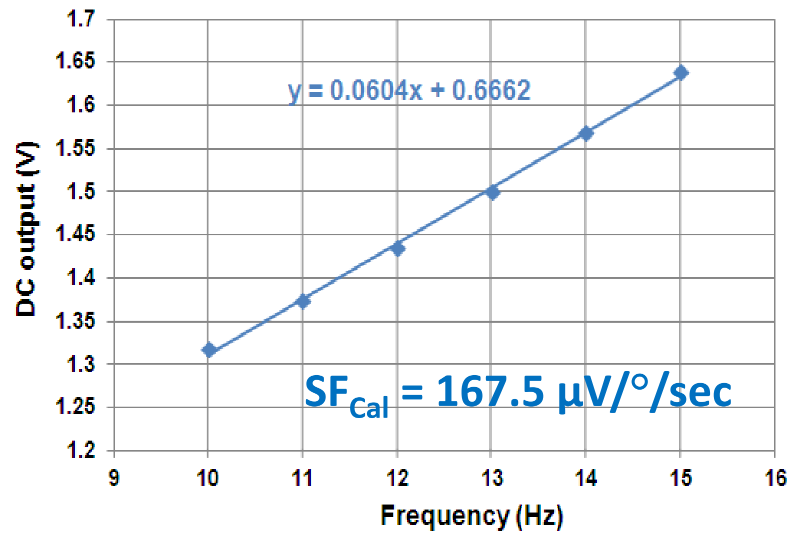

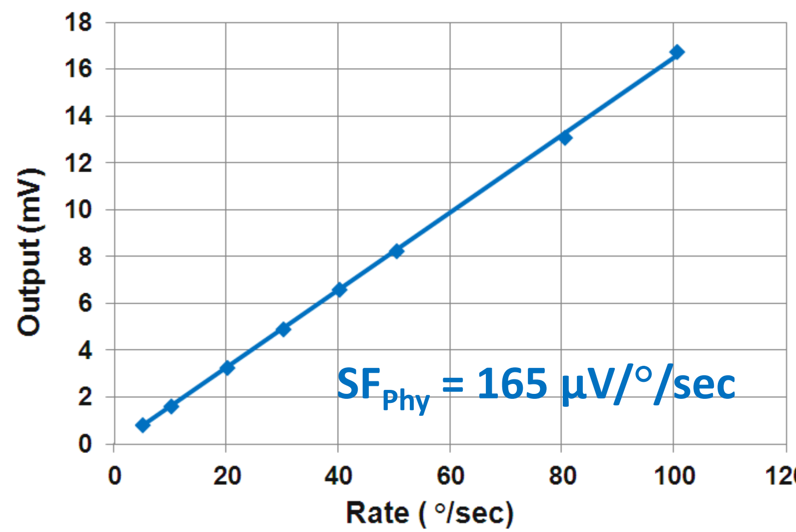

- Staircase is generated as the output of electrostatic rotation at different frequencies.

Automatic Mode-Matching
and
Quadrature Cancellation

Automatic Mode-matching – Maximum ZRO

- Minimum frequency split happens at maximum quadrature amplitude

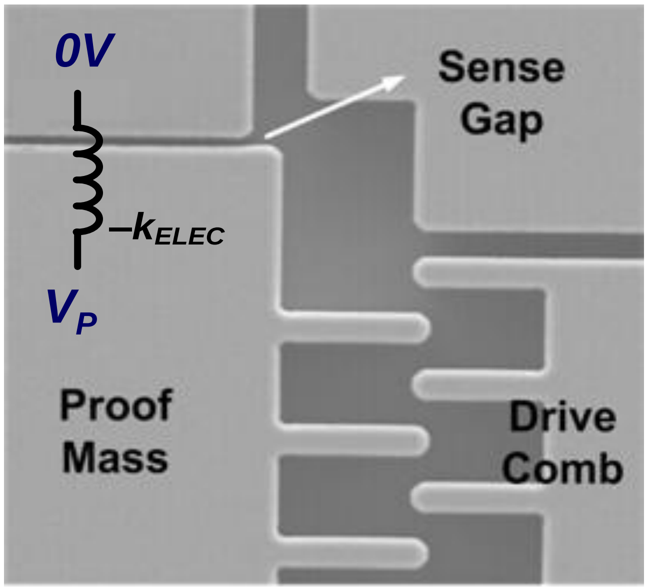

$$\omega_{SNS} = \sqrt{\frac{K_{y-mech} - \sum_{i=1}^{N} \frac{\varepsilon_o A_i}{d_{oi}^3} V_{P-i}^2}{M_{eff}}}$$

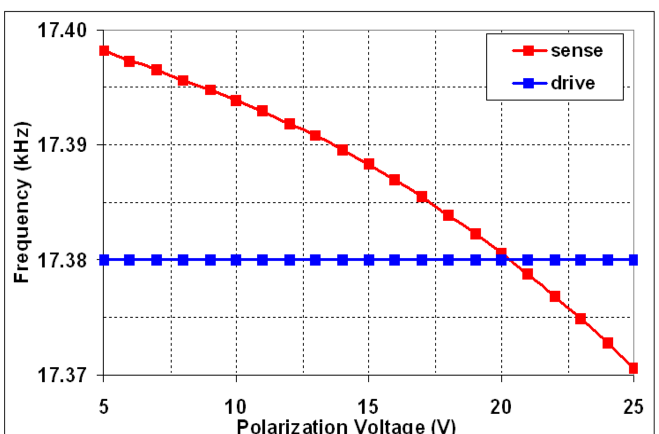

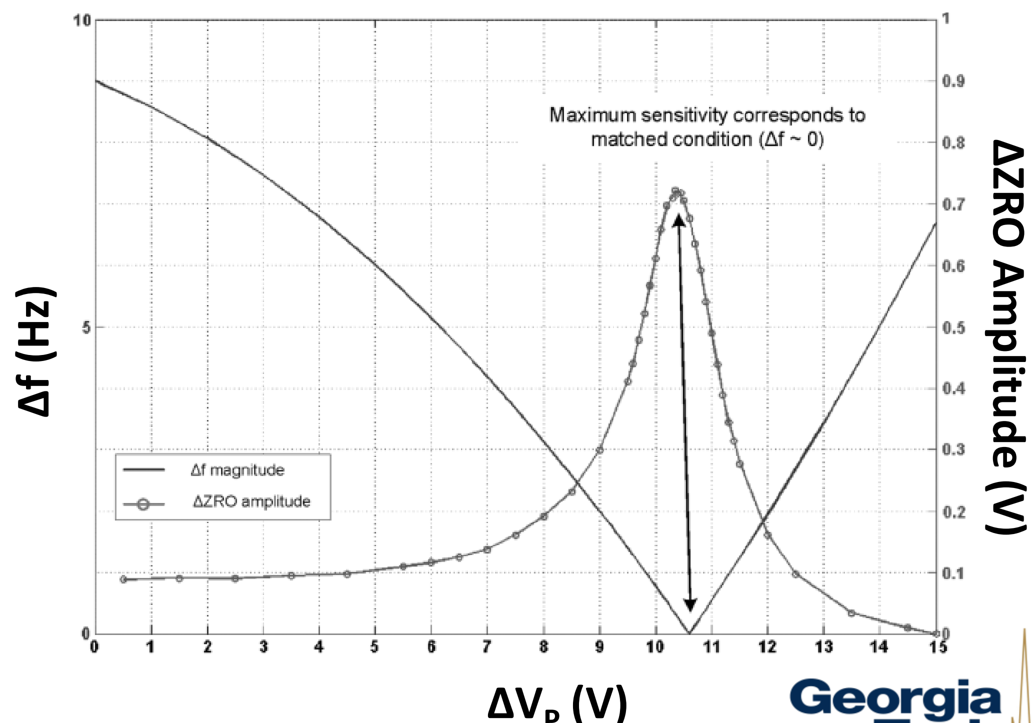

[Sharma et al, JSSC 2009]

System Architecture

- $f_{SNS} > f_{drv}$ enables mode-matching using spring softening through V_P
- Maxima of ZRO is achieved in a close loop mode-matching system

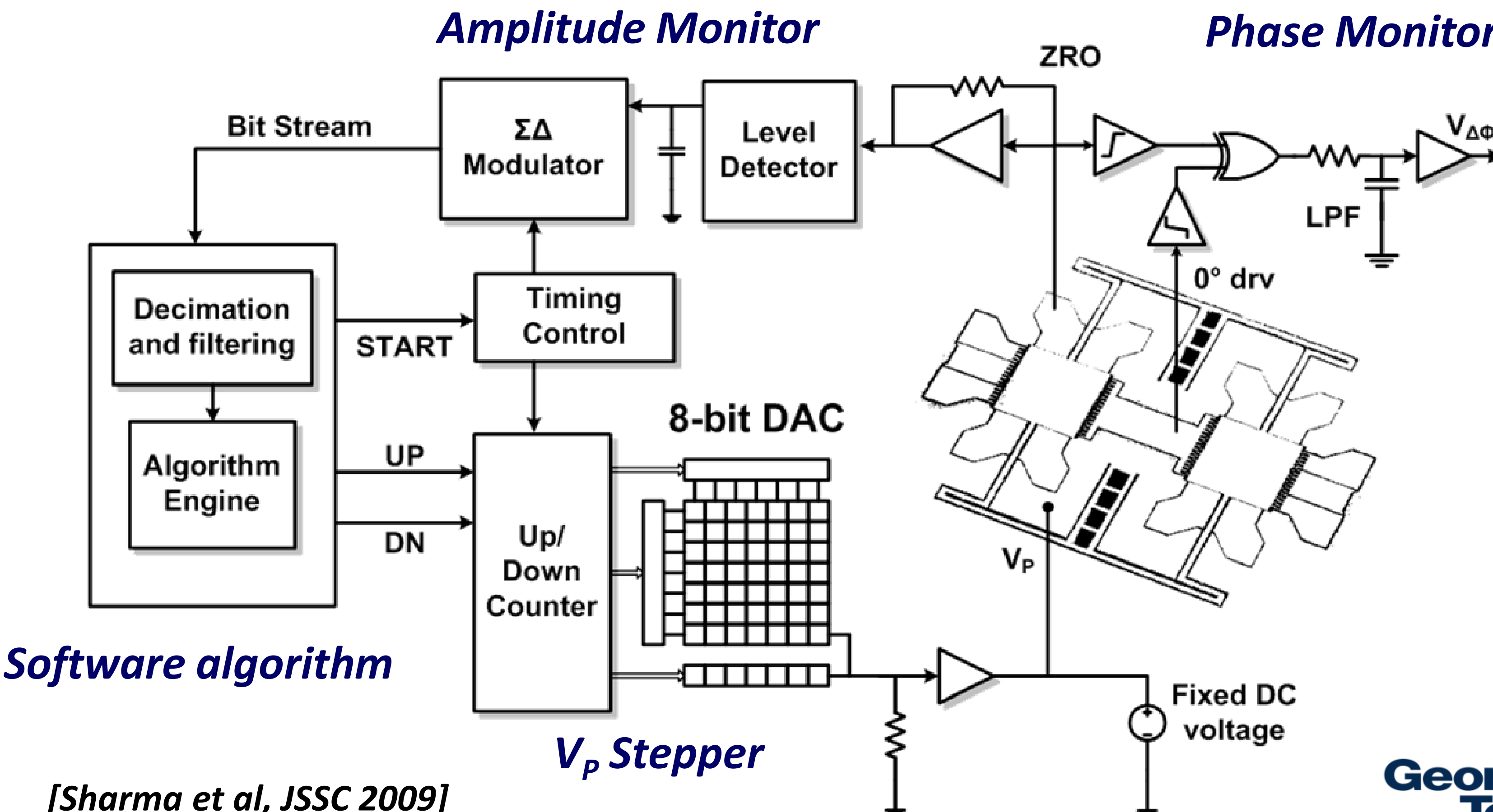

[Sharma et al, JSSC 2009]

Georgia Tech

Extremum Seeking Control

- Maximize the amplitude of motion along the sense
- Perturbation signal at ω modulates the DC control signals for faster operation

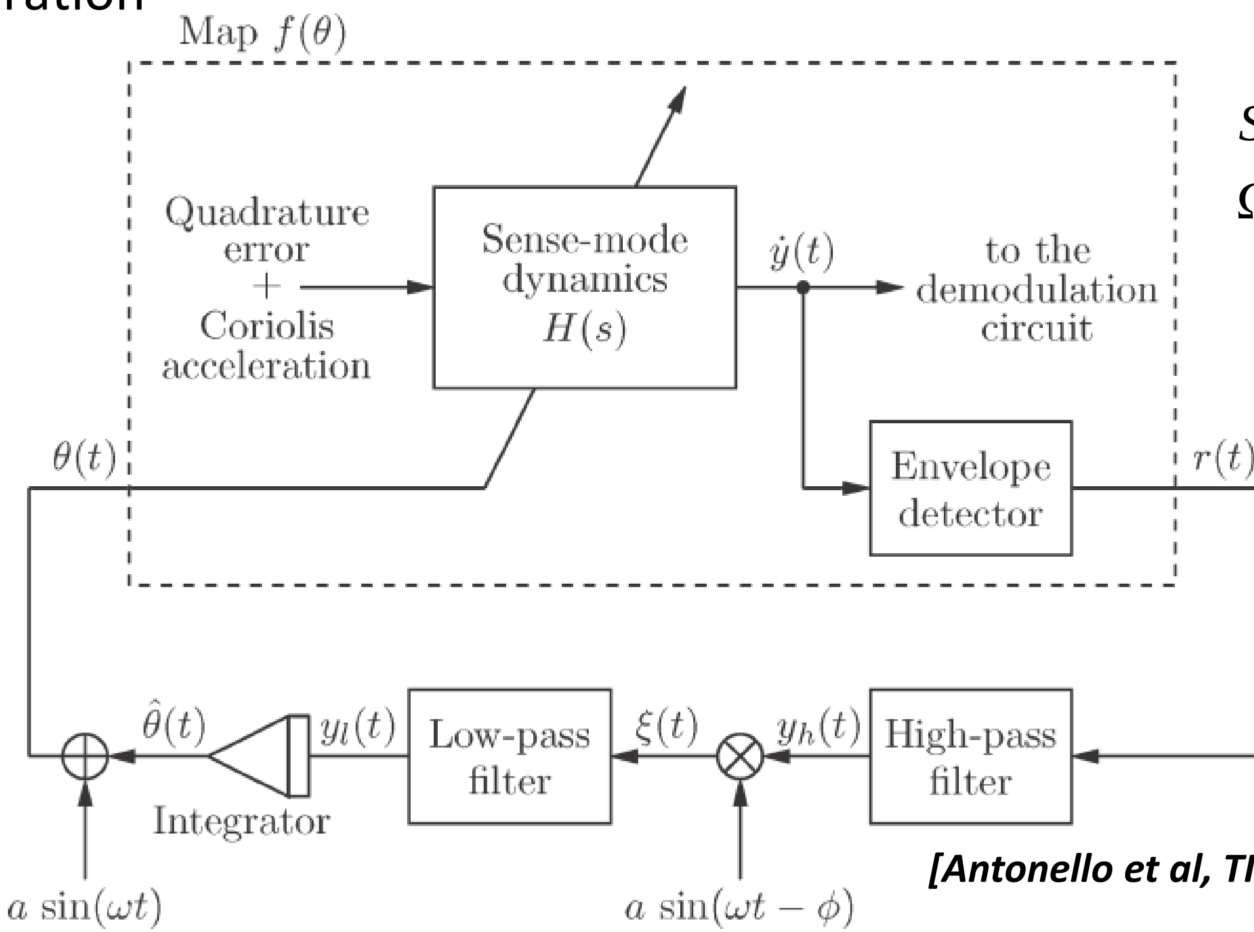

Stability condition :

$\Omega_z \ll \omega_c \ll \omega_0$

[Antonello et al, TIE 2009]

Automatic Mode-matching – Dual Pilot Tones

- Two pilot tones at equal offset from drive-mode resonance frequency are used to excite the sense mode.
- At mode-matched condition, the amplitude of the two tones is equal.

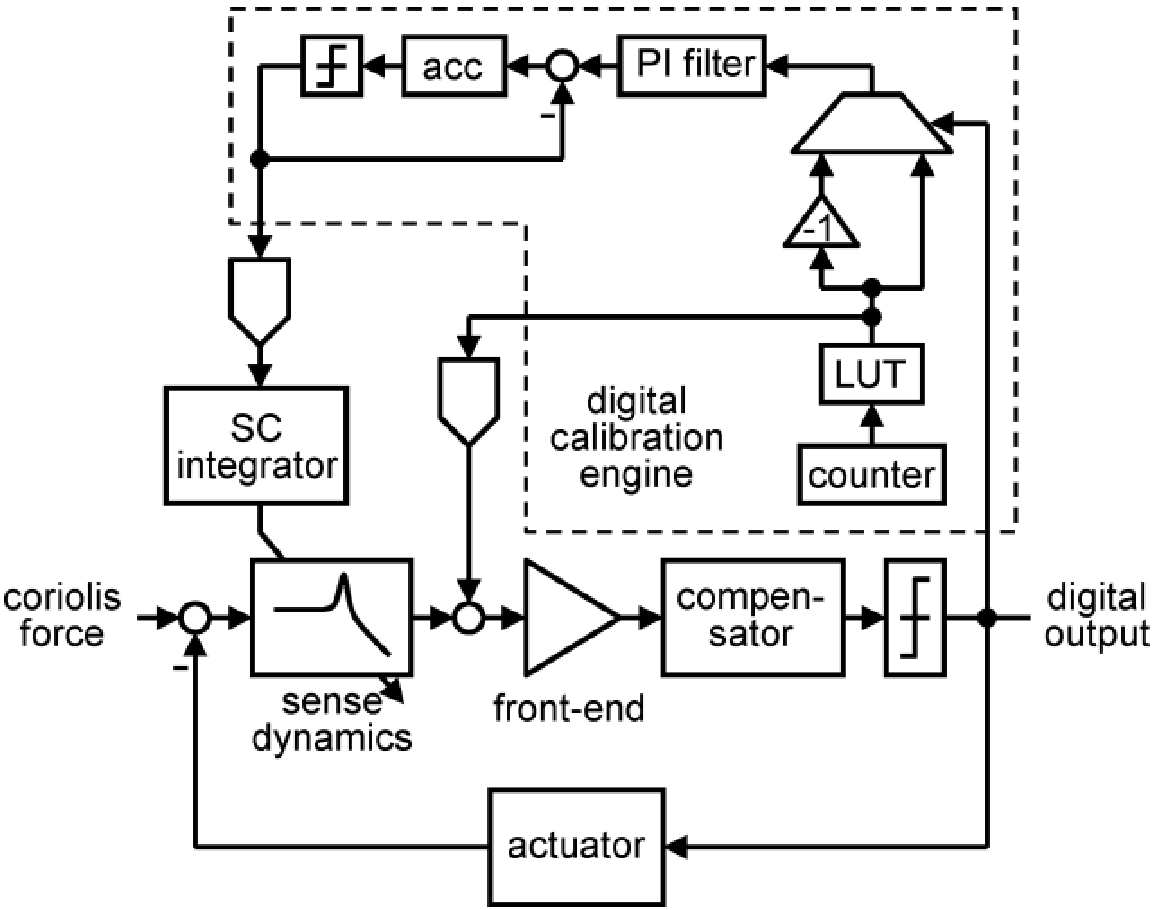

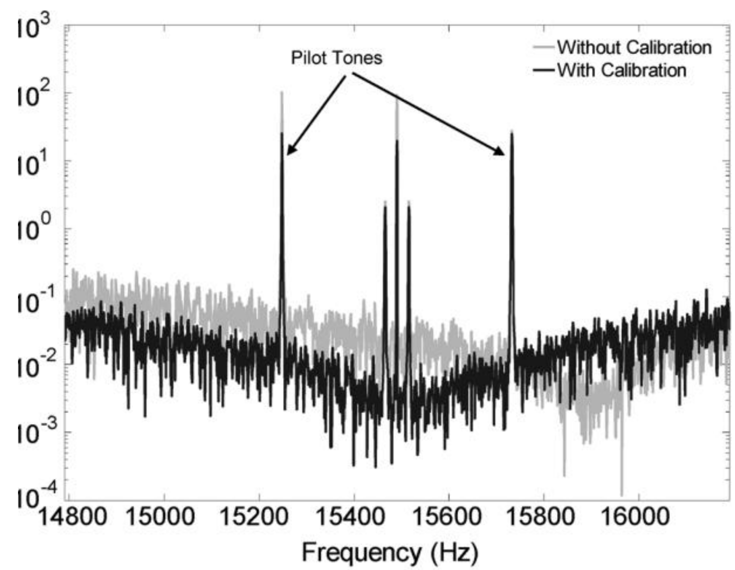

Pilot tones at 250Hz offset

[Ezekwe et al, JSSC 2008]

Georgia Tech

Mode-matching – Phase-Domain Control

- Both drive and sense modes are excited
- Phase difference of sense and drive outputs generates an error signal
- Mode-matching can be maintained while rate is being detected.

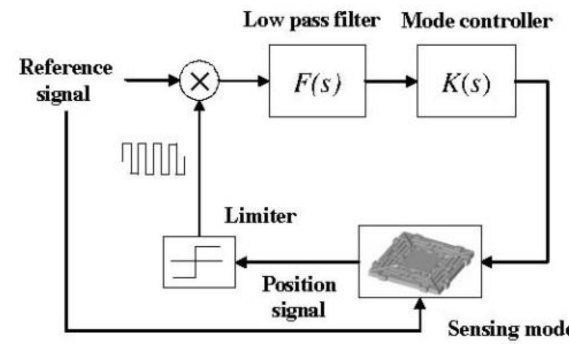

Mode-matching control loop

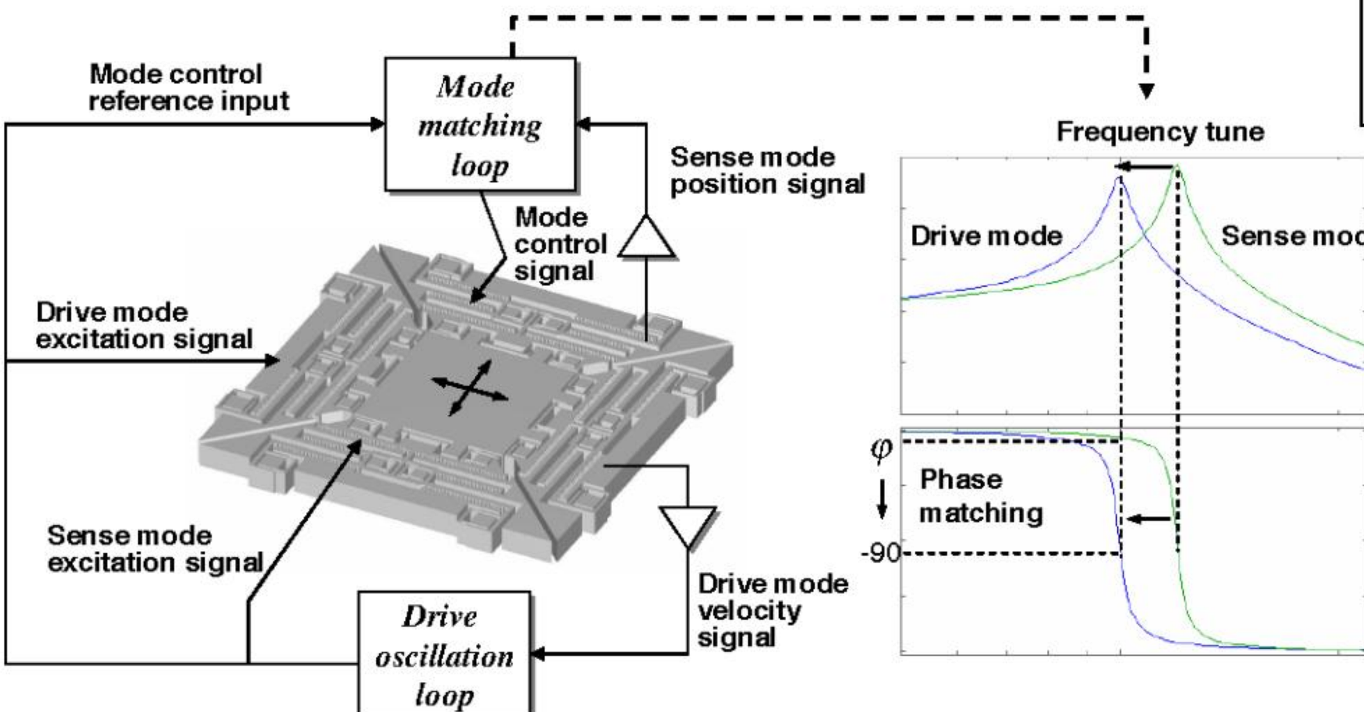

[Sung et al, Transactions on Mechatronics 2009]

Offline Phase-based Mode-matching

- In stationary mode, the phase difference of the sense and drive signals is kept fixed at 90°
- In rate detection mode, mode-matching cannot be monitored anymore

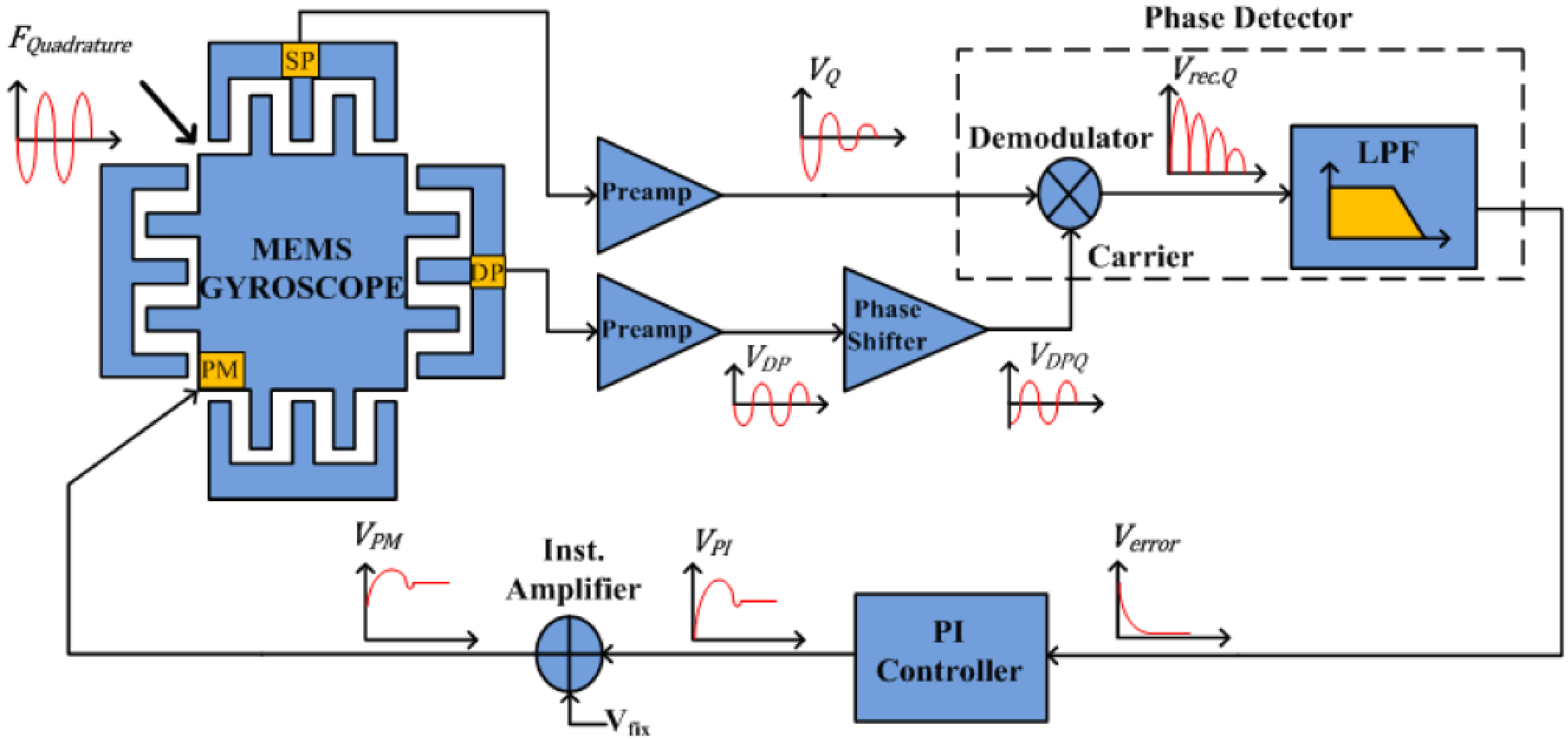

[Sonmezoglu et al, MEMS 2012]

Georgia Tech

Open-Loop Quadrature Cancellation

- Ideally at mode-matched condition: demodulate quadrature error and subtract from sense output current
  - Noise injection to sense front-end
- ZRO is not necessarily quadrature-phase!
  - In-phase component results in offset

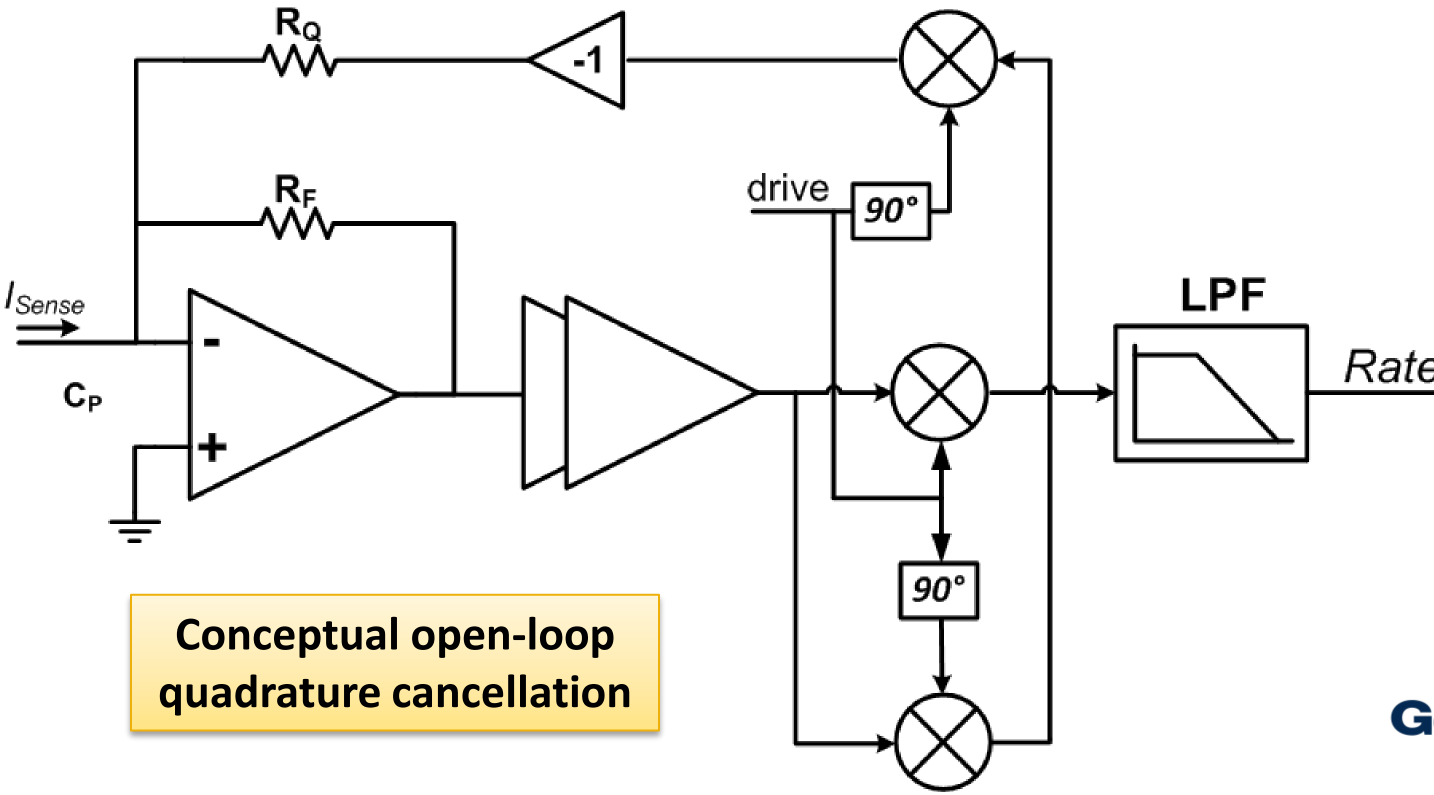

Conceptual open-loop quadrature cancellation

Closed-Loop Quadrature Compensation

- Demodulate quadrature error, and feedback a DC voltage to fix the undesired gyroscope displacement.
- In-phase ZRO term will appear as an offset.

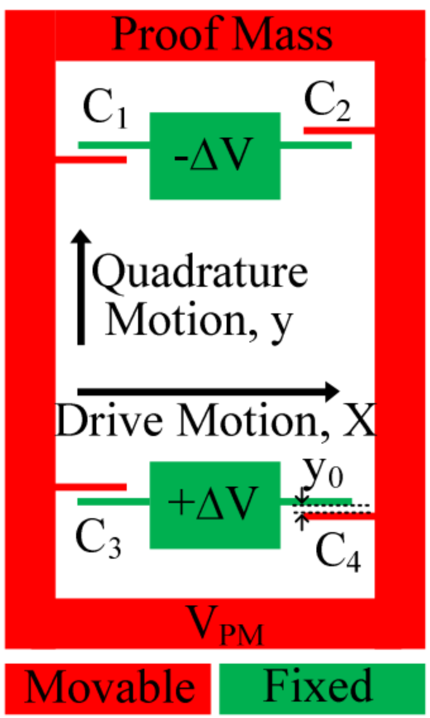

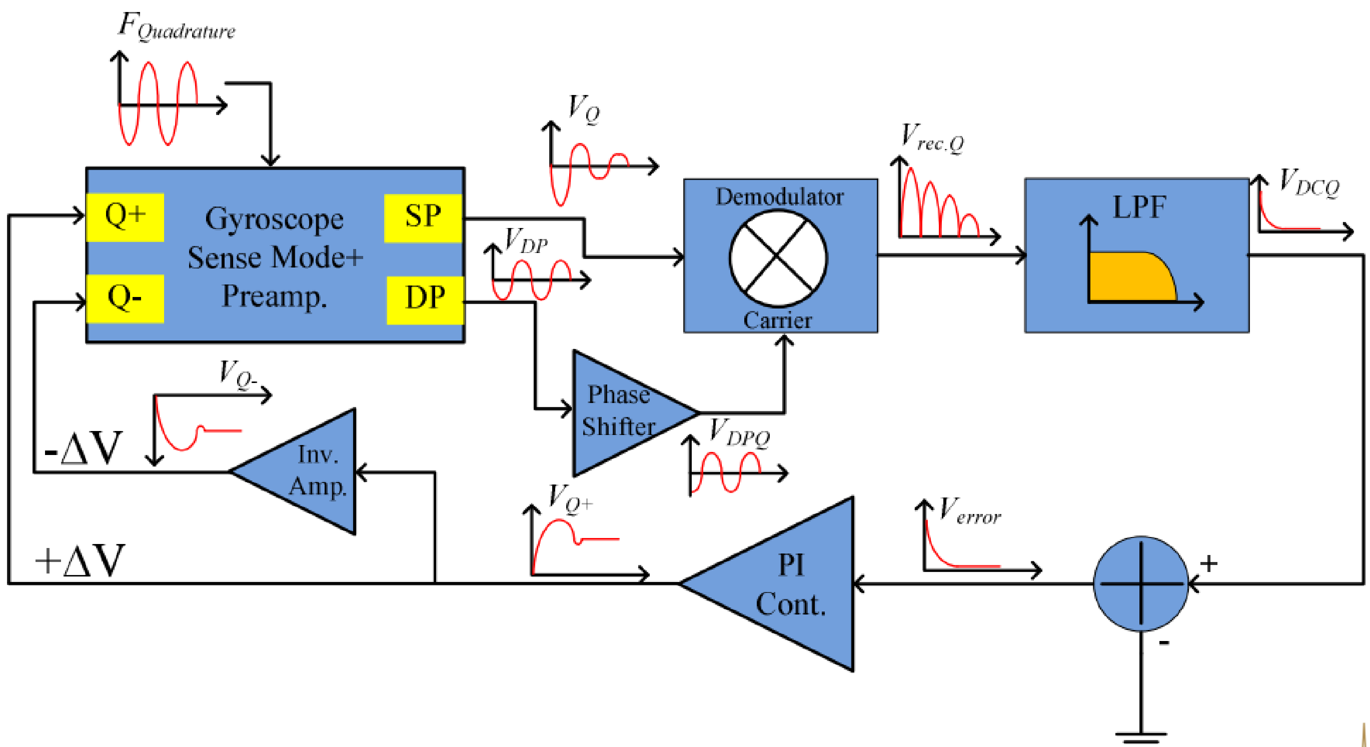

[Tatar et al, MEMS 2011]

Conclusions

- **MEMS does the sensing, Circuits do the thinking!**
- Smart system architecture and careful circuit design are needed to show the true color of high-performance inertial MEMS technology.
- Self-calibration algorithms and architectures are needed to compensate for environmental effects and long-term drifts in MEMS inertial sensors.
- Automatic real-time mode-matching and quadrature compensation are essential parts of interface systems for high-performance navigation-grade MEMS gyroscopes.

References

[1] N. Yazdi, F. Ayazi, and K. Najafi, “Micromachined inertial sensors,” *Proc. IEEE*, vol. 86, no. 8, pp. 1640–1659, Aug. 1998.

[2] A. Sharma, M. Zaman, and F. Ayazi, “A 104-dB dynamic range transimpedance-based CMOS ASIC for tuning fork microgyroscopes,” *Solid-State Circuits, IEEE Journal of* , vol. 42, no. 8, pp. 1790-1802, Aug. 2007.

[3] M. F. Zaman, A. Sharma, Z. Hao, and F. Ayazi, "A mode-matched silicon-yaw tuning-fork gyroscope with subdegree-per-hour Allan deviation bias instability," *Microelectromechanical Systems, Journal of,* vol. 17, pp. 1526-1536, 2008.

[4] J. A. Geen, S. J. Sherman, J. F. Chang, and S. R. Lewis, “Single-Chip Surface Micromachined Integrated Gyroscope with 50°/h Allan Deviation,” *Solid-State Circuits*, *IEEE Journal of,* vol. 37, no. 12, pp. 1860-1866, Dec. 2002.

[5] M. S. Weinberg and A. Kourepenis, “Error sources in in-plane silicon tuning-fork MEMS gyroscopes,” *Microelectromechanical Systems, Journal of,* vol. 15, no. 3, pp. 479–491, Jun. 2006.

[6] L. Prandi, C. Caminada, L. Coronato, G. Cazzaniga, F. Biganzoli, R. Antonello, R. Oboe, "A low-power 3-axis digital-output MEMS gyroscope with single drive and multiplexed angular rate readout,"*Solid-State Circuits Conference Digest of Technical Papers (ISSCC), 2011 IEEE International*, pp.104,106, 20-24 Feb. 2011.

[7] Seeger, J., Lim, M., & Nasiri, S. (2010). Development of High-Performance, High-Volume Consumer MEMS Gyroscopes. In *Technical Digest Solid-State Sensor, Actuator and Microsystems Workshop, Hilton Head Island* (pp. 61-64).

[8] A. A. Seshia, R. T. Howe, S. Montague, "An integrated microelectromechanical resonant output gyroscope," *Micro Electro Mechanical Systems, 2002. The Fifteenth IEEE International Conference on*, pp.722,726, 24-24 Jan. 2002.

Georgia Tech

References

[9] V. P. Petkov, B. E. Boser, "A fourth-order ΣΔ interface for micromachined inertial sensors," *Solid-State Circuits, IEEE Journal of* , vol.40, no.8, pp.1602,1609, Aug. 2005.

[10] M. H. Kline, Y. Yeh, B. Eminoglu, H. Najar, M. Daneman, D. A. Horsley, B. E. Boser, "Quadrature FM gyroscope," *Micro Electro Mechanical Systems (MEMS), 2013 IEEE 26th International Conference on*, pp.604,608, 20-24 Jan. 2013.

[11] G. Casinovi, W. K. Sung, M. Dalal, A. N.-Shirazi, F. Ayazi, "Electrostatic self-calibration of vibratory gyroscopes," *Micro Electro Mechanical Systems (MEMS), 2012 IEEE 25th International Conference on*, pp.559,562, Jan. 29 2012-Feb. 2 2012.

[12] A. N. Shirazi, G. Casinovi, M. Dalal, F. Ayazi, "Combined phase-readout and self-calibration of MEMS gyroscopes," *Solid-State Sensors, Actuators and Microsystems (TRANSDUCERS & EUROSENSORS XXVII), 2013 Transducers & Eurosensors XXVII: The 17th International Conference on*, pp.960,963, 16-20 June 2013.

[13] A. Sharma, M. F. Zaman, and F. Ayazi, “A Sub 0.2°/hr Bias Drift Micromechanical Gyroscope with Automatic CMOS Mode-Matching,” IEEE J. of Solid-State Circuits, Vol. 44, No.5, pp. 1593-1608, May 2009.

[14] C. D. Ezekwe, B. E. Boser, "A Mode-Matching ΣΔ Closed-Loop Vibratory Gyroscope Readout Interface With a 0.004 /s/ √Hz Noise Floor Over a 50 Hz Band," *Solid-State Circuits, IEEE Journal of* , vol.43, no.12, pp.3039,3048, Dec. 2008.

[15] R. Antonello, R. Oboe, L. Prandi, F. Biganzoli, "Automatic Mode Matching in MEMS Vibrating Gyroscopes Using Extremum-Seeking Control," *Industrial Electronics, IEEE Transactions on* , vol.56, no.10, pp.3880,3891, Oct. 2009.

[16] M. Saukoski, L. Aaltonen, K. A. Halonen, "Zero-Rate Output and Quadrature Compensation in Vibratory MEMS Gyroscopes," *Sensors Journal, IEEE* , vol.7, no.12, pp.1639,1652, Dec. 2007.

References

[17] S. Sung, W. T. Sung, C. Kim, S. Yun, Y. J. Lee, "On the Mode-Matched Control of MEMS Vibratory Gyroscope via Phase-Domain Analysis and Design," *Mechatronics, IEEE/ASME Transactions on* , vol.14, no.4, pp.446,455, Aug. 2009.

[18] S. Sonmezoglu, S. E. Alper, T. Akin, "An automatically mode-matched MEMS gyroscope with 50 Hz bandwidth," *Micro Electro Mechanical Systems (MEMS), 2012 IEEE 25th International Conference on*, pp.523,526, Jan. 29 2012-Feb. 2 2012.

[19] J. Seeger, A. J. Rastegar, M. T. Tormey, "Method and apparatus for electronic cancellation of quadrature error," US Patent, 0180908 A1, August 9, 2007.

[20] R. Antonello, R. Oboe, L. Prandi, C. Caminada, F. Biganzoli, "Open-loop compensation of the quadrature error in MEMS vibrating gyroscopes," *Industrial Electronics, 2009. IECON '09. 35th Annual Conference of IEEE*, pp.4034,4039, 3-5 Nov. 2009.

[21] E. Tatar, S. E. Alper, T. Akin, "Effect of quadrature error on the performance of a fully-decoupled MEMS gyroscope," *Micro Electro Mechanical Systems (MEMS), 2011 IEEE 24th International Conference on*, pp.569,572, 23-27 Jan. 2011.